European Journal of Inorganic Chemistry

Supporting Information

Ligand Exchange Triggered Photosensitizers – Bodipy-Tagged NHC-Metal Complexes for Conversion of $^3O_2$ to $^1O_2$

Stepan Popov and Herbert Plenio*

Table of contents

Materials. All chemicals were purchased as reagent grade from commercial suppliers and used without further purification unless otherwise noted. DCM was obtained from Fisher Scientific and pentane was obtained from BCD Chemie GmbH in Frankfurt. All solvents were stored over molecular sieves (4 Å) under N_2. Preparative chromatography was performed using Merck silica 60 (0.063 – 0.02 mesh). *Meso*-Cl BODIPY was synthesized according to the literature procedure [1].

Figure S1. Home-built photoreactor for photocatalytic experiments.

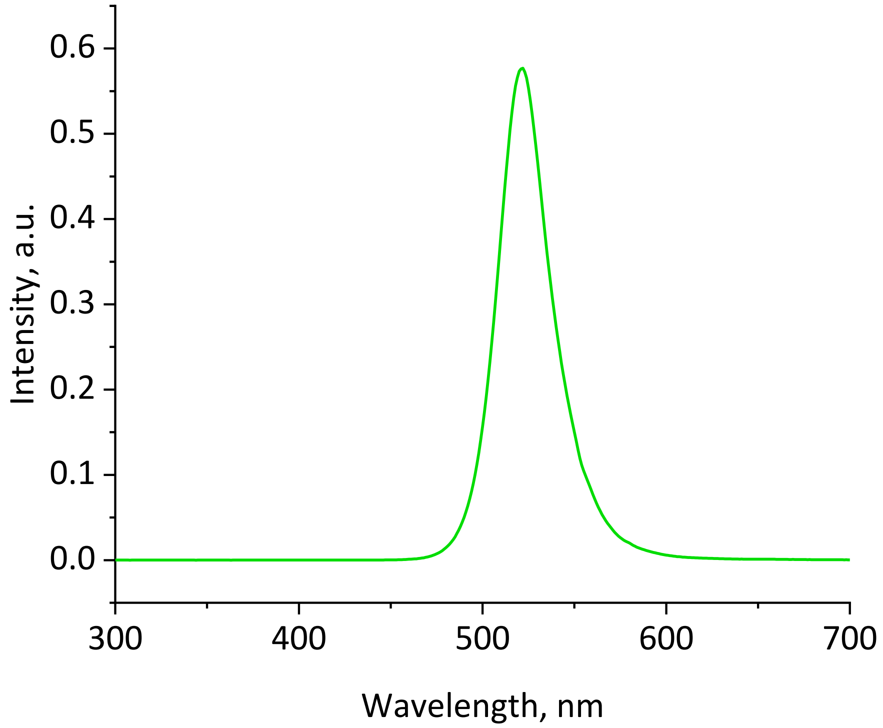

Figure S2. Light intensity spectrum of the green LED system used in photocatalysis experiment.

UV/Vis measurements

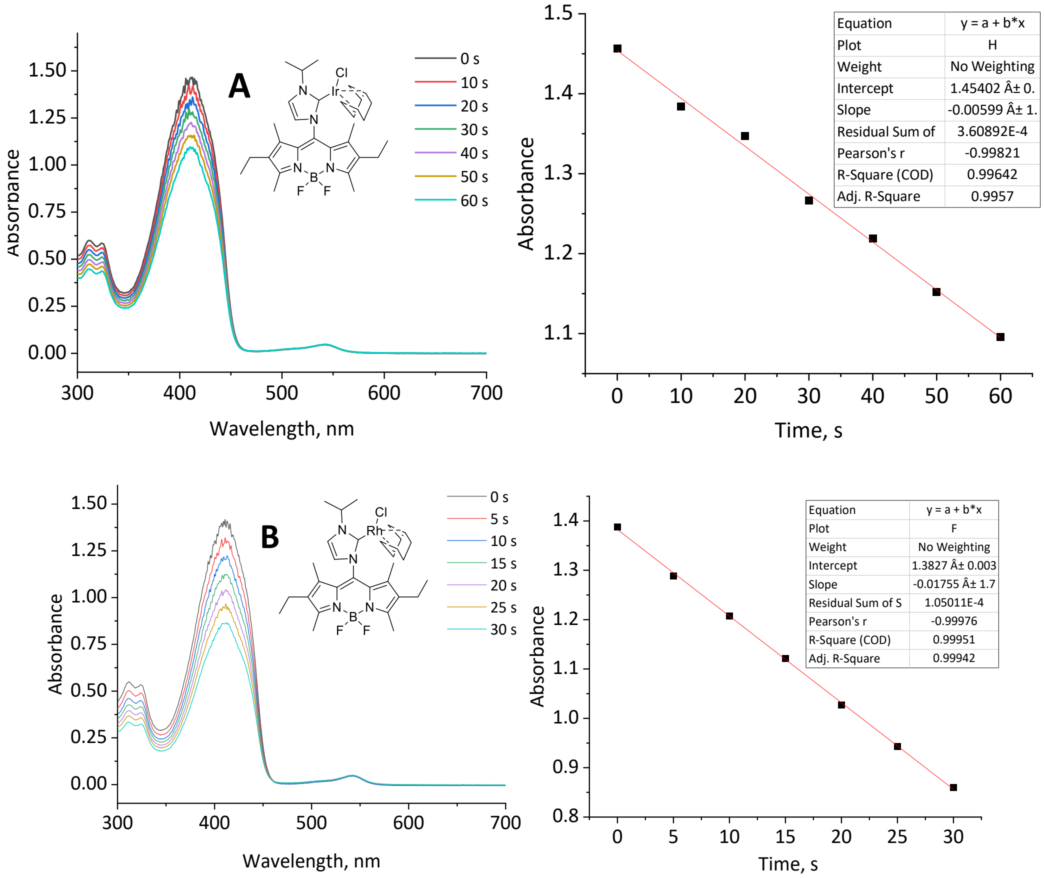

Figure S3. Left: ***A***: Decay of the DPBF (c_0 = 90 μM) in a presence of [IrCl(cod)(**3**)] (c = 1.0 μM) in CH_3CN in the absorption spectra. ***B***: Decay of the DPBF (c_0 = 90 μM) in a presence of [RhCl(cod)(**3**)] (c = 1.0 μM) in CH_3CN. Solutions were irradiated with a green LED. Right: Linear regression for a decreasing of the absorbance at 410 nm for ***A*** and ***B***.

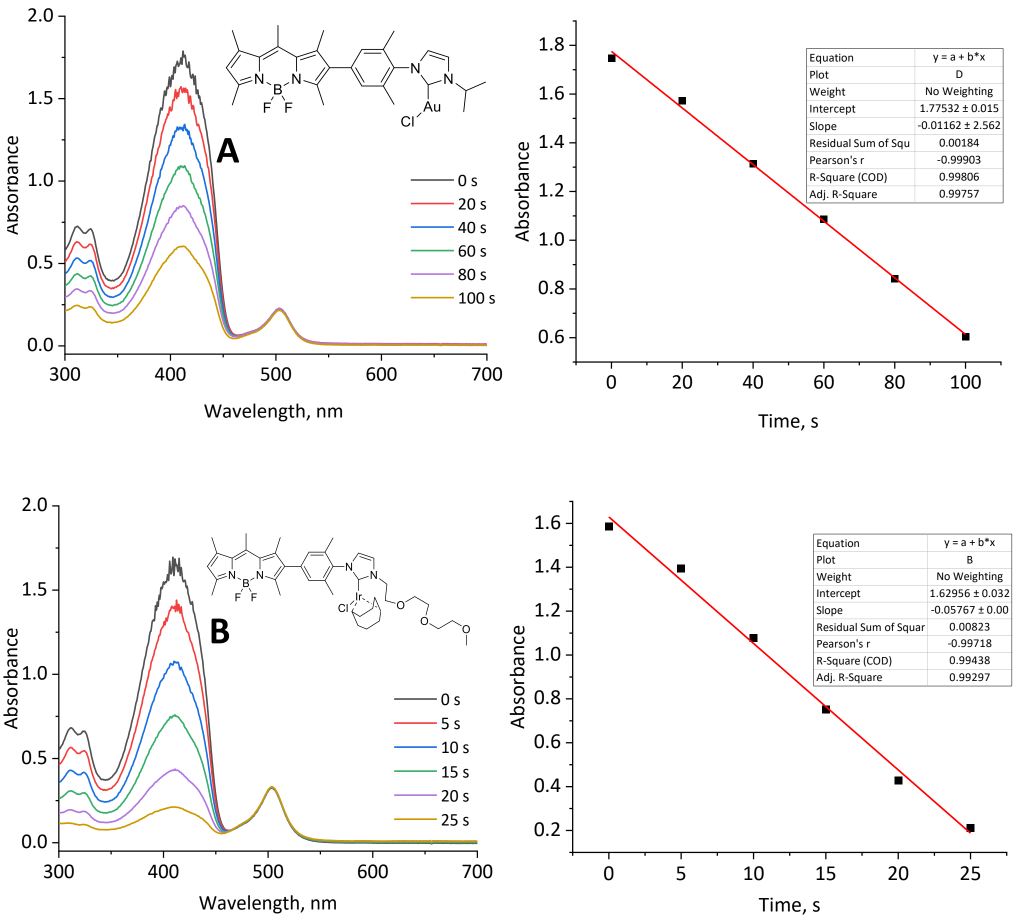

Figure S4. Left: ***A***: Decay of the DPBF (c_0 = 90 μM) in a presence of [AuCl(NHC_PK)] (c = 5.0 μM) in CH_3CN in the absorption spectra. ***B***: Decay of the DPBF (c_0 = 90 μM) in a presence of [IrCl(cod)(NHC_PK1)] (c = 5.0 μM) in CH_3CN. Solutions were irradiated with a green LED. Right: Linear regression for a decreasing of the absorbance at 410 nm for ***A*** and ***B***..

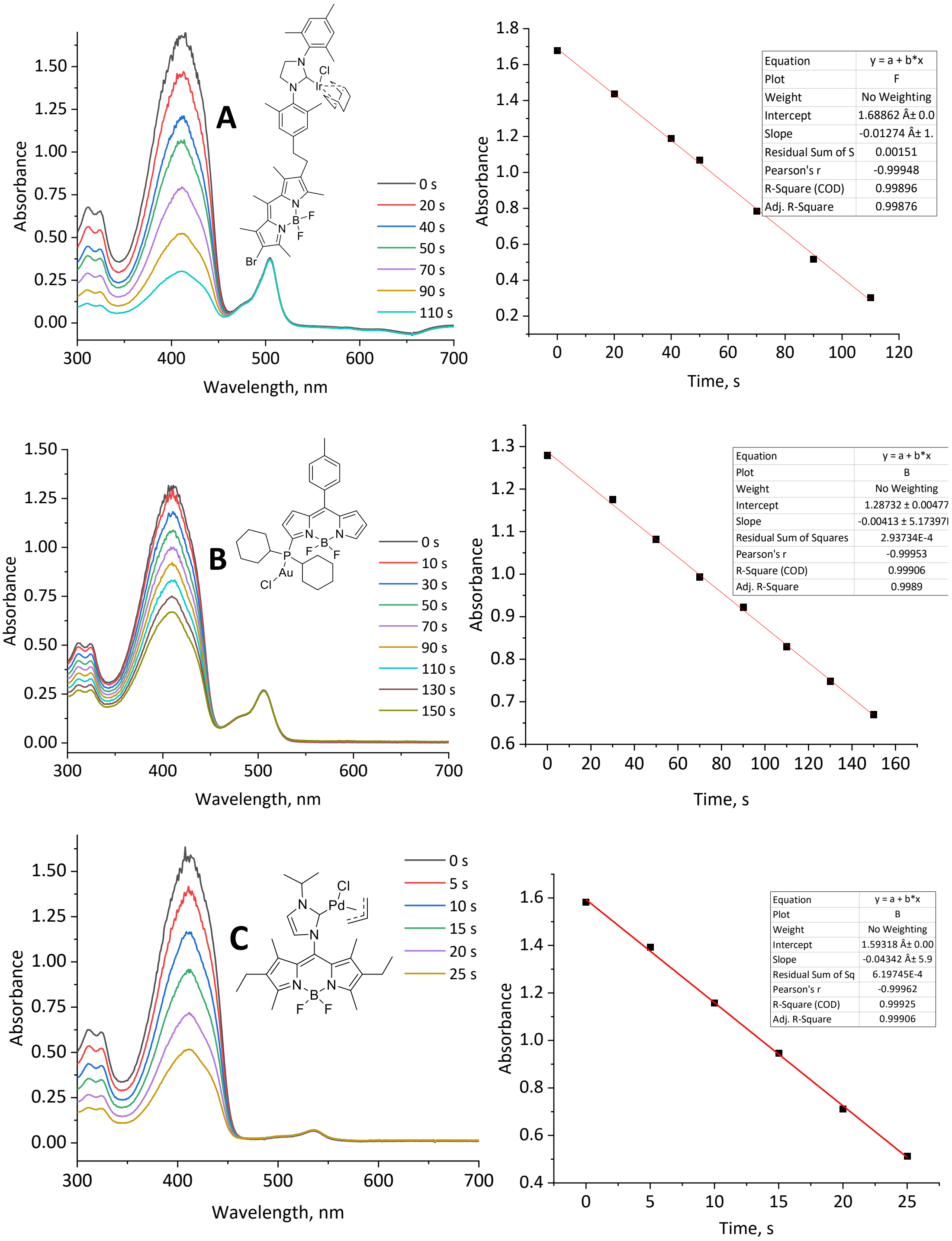

Figure S5. Left: ***A***: Decay of the DPBF (c_0 = 90 μM) in a presence of [IrCl(cod)(NHC_PK2)] (*c* = 5.0 μM) in CH_3CN in the absorption spectra. ***B***: Decay of the DPBF (c_0 = 90 μM) in a presence of [AuCl(Cy_2P-bdp)] (*c* = 5.0 μM) in CH_3CN. ***C***: Decay of the DPBF (c_0 = 90 μM) in a presence of [PdCl(allyl)(**3**)] (*c* = 1.0 μM) in CH_3CN. Solutions were irradiated with a green LED. Right: Linear regressions for a decreasing of the absorbance at 410 nm for ***A,B*** and ***C.***

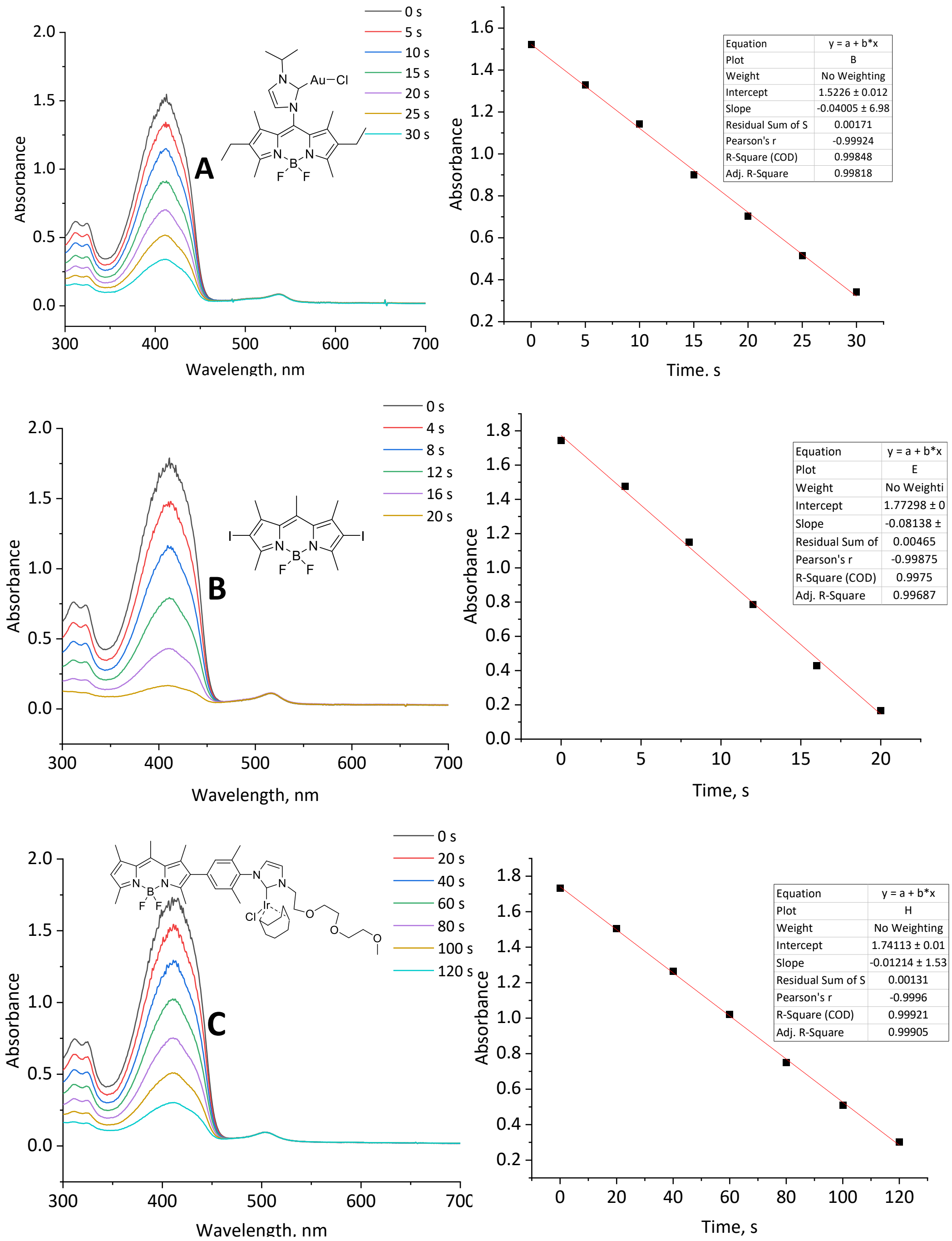

Figure S6. Left: ***A***: Decay of the DPBF (c_0 = 90 μM) in a presence of [AuCl(**3**)] (c = 1.0 μM) in CH_3CN in the absorption spectra. ***B***: Decay of the DPBF (c_0 = 90 μM) in a presence of 2,6-diiodo-BODIPY (c = 1.0 μM) in CH_3CN. ***C***: Decay of the DPBF (c_0 = 90 μM) in a presence of [IrCl(cod)(NHC_PK1)] (c = 1.0 μM) in CH_3CN. Solutions were irradiated with a green LED. Right: Linear regressions for a decreasing of the absorbance at 410 nm for ***A***, ***B*** and ***C***.

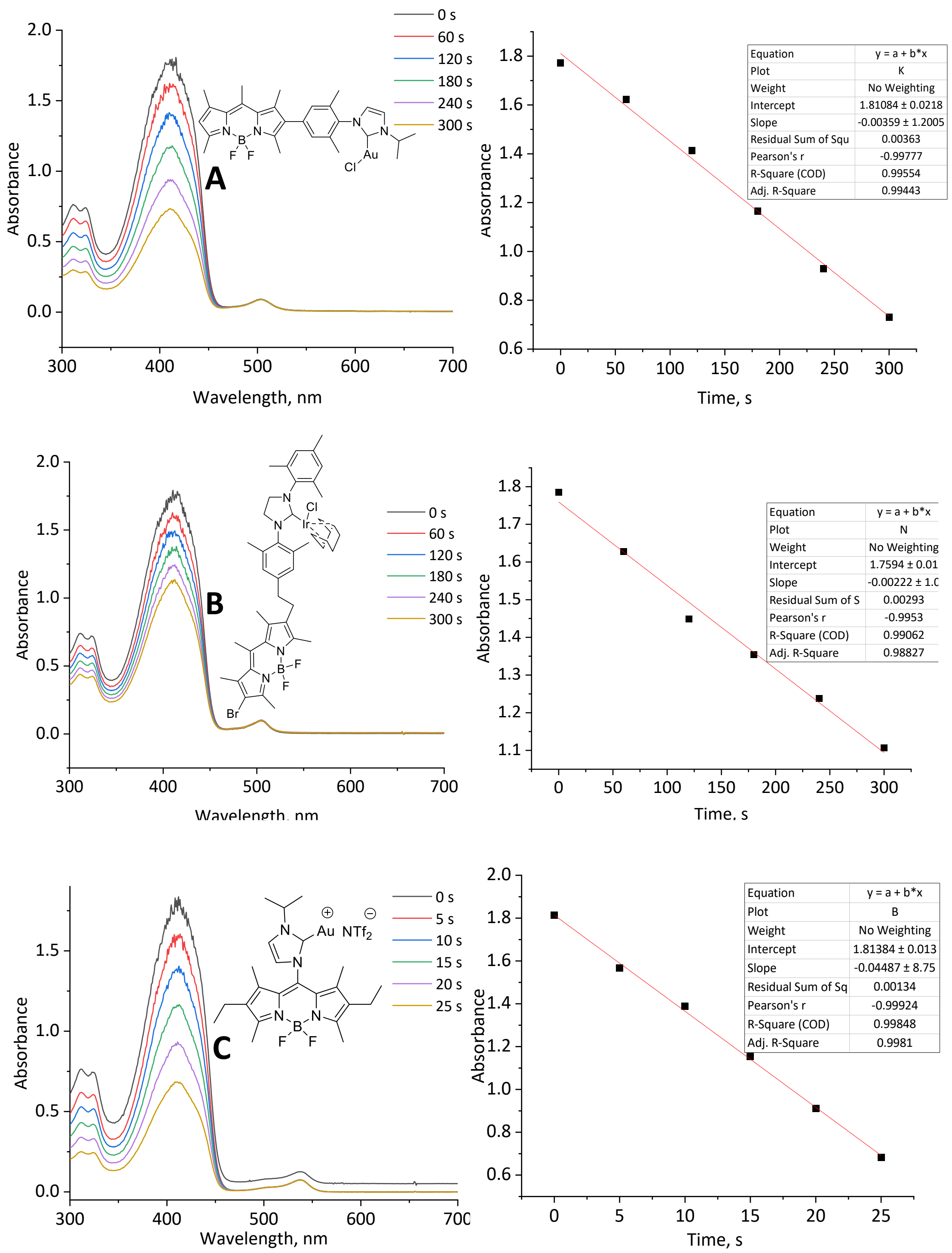

Figure S7. Left: ***A***: Decay of the DPBF (c_0 = 90 μM) in a presence of [AuCl(NHC_PK)] (c = 1.0 μM) in CH_3CN in the absorption spectra. ***B***: Decay of the DPBF (c_0 = 90 μM) in a presence of [IrCl(cod)(NHC_PK2)] (c = 1.0 μM) in CH_3CN. ***C***: Decay of the DPBF (c_0 = 90 μM) in a presence of [AuNTf$_2$(**3**)] (c = 1.0 μM) in CH_3CN. Solutions were irradiated with a green LED. Right: Linear regressions for a decreasing of the absorbance at 410 nm for ***A***, ***B*** and ***C***.

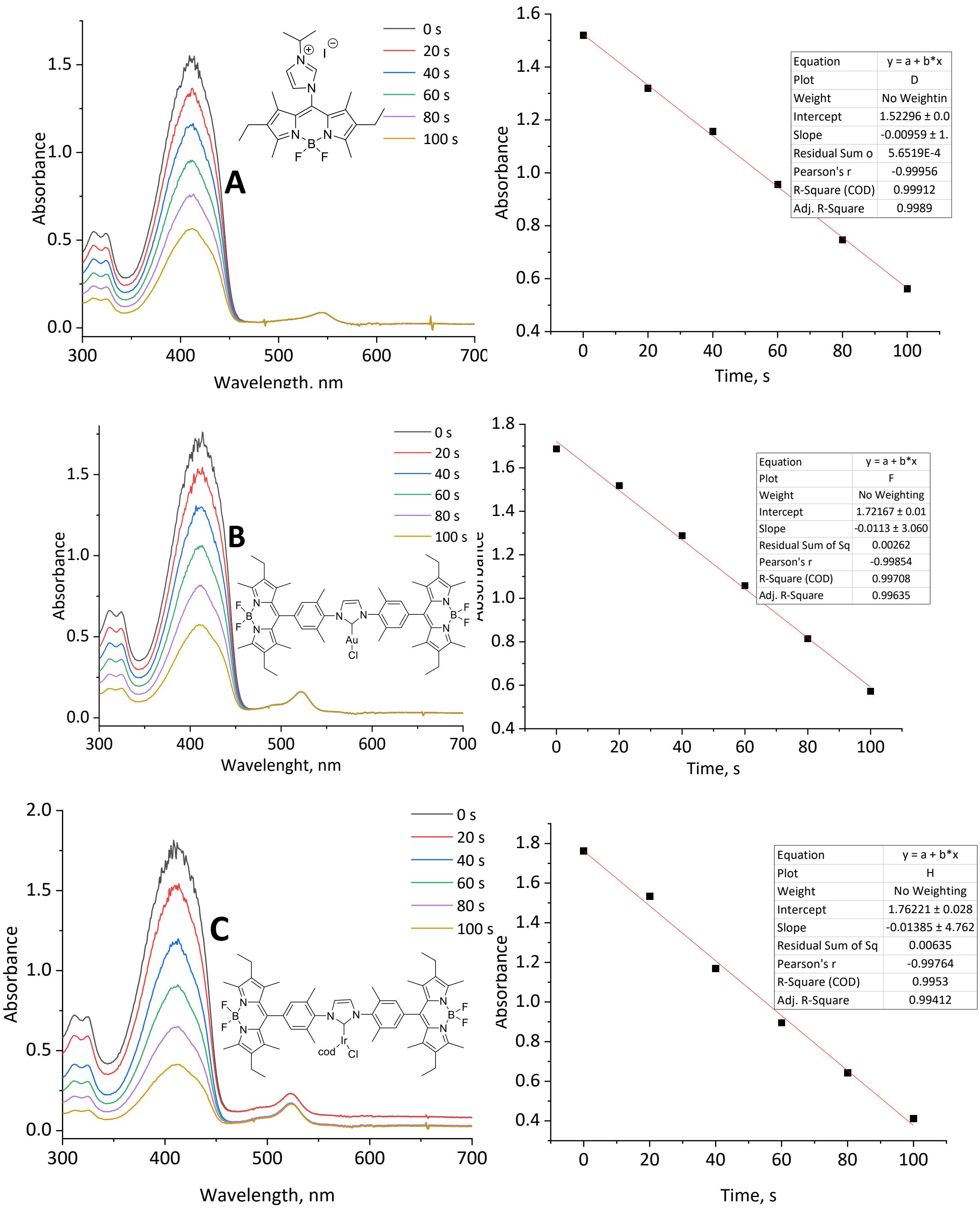

Figure S8. Left: ***A***: Decay of the DPBF (c_0 = 90 μM) in a presence of BODIPY imidazolium salt **3** (c = 1.0 μM) in CH_3CN in the absorption spectra. ***B***: Decay of the DPBF (c_0 = 90 μM) in a presence of [AuCl(NHC_OH1)] (c = 1.0 μM) in CH_3CN. ***C***: Decay of the DPBF (c_0 = 90 μM) in a presence of [IrCl(cod)(NHC_OH1)] (c = 1.0 μM) in CH_3CN. Solutions were irradiated with a green LED. Right: Linear regressions for a decreasing of the absorbance at 410 nm for ***A***, ***B*** and ***C***

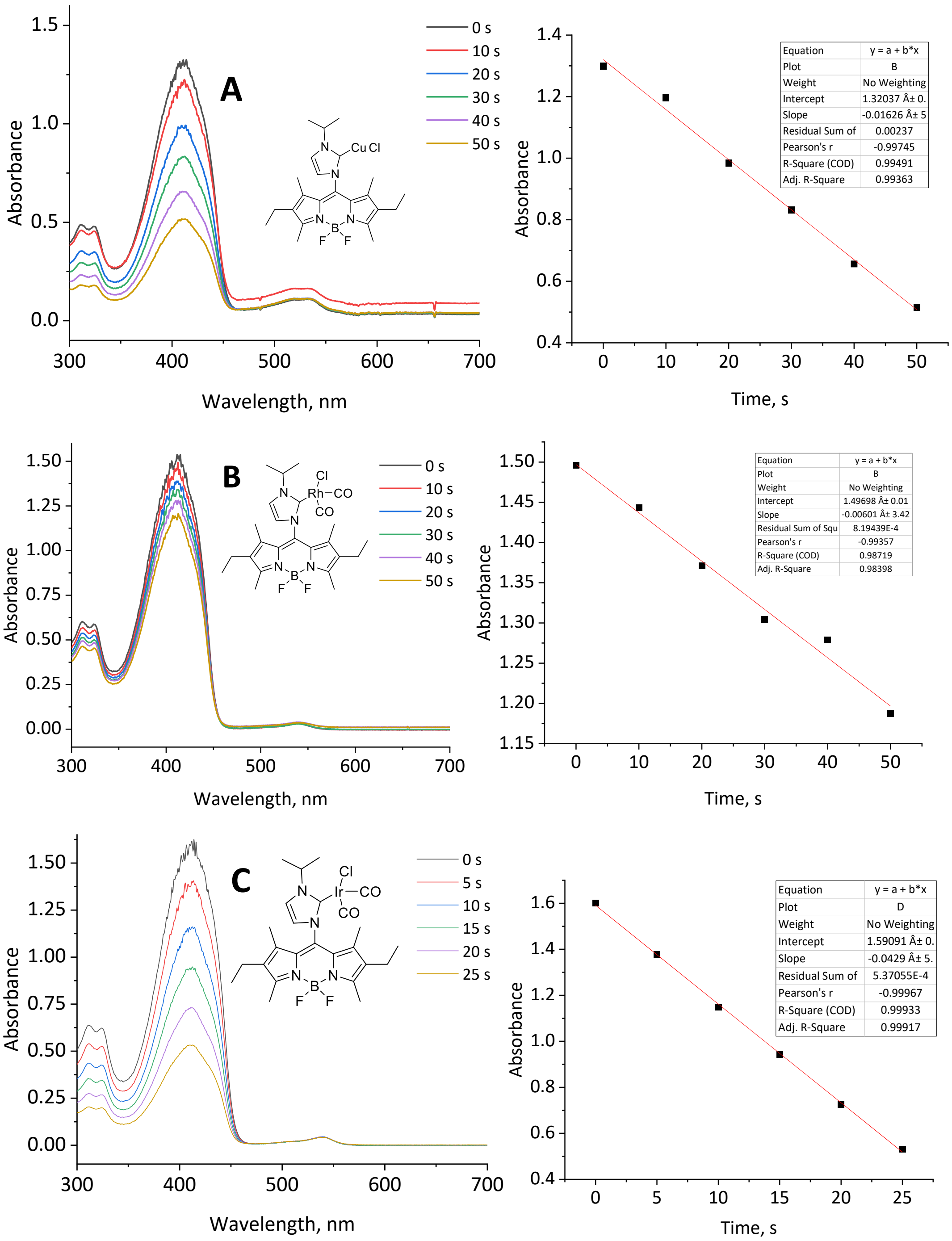

Figure S9. Left: ***A***: Decay of the DPBF (c_0 = 90 μM) in a presence of of [CuCl(**3**)] (c = 1.0 μM) in CH_3CN in the absorption spectra. ***B***: Decay of the DPBF (c_0 = 90 μM) in a presence of [RhCl(CO)$_2$(**3**)] (c = 1.0 μM) in CH_3CN. ***C***: Decay of the DPBF (c_0 = 90 μM) in a presence of of [IrCl(CO)$_2$(**3**)] (c = 1.0 μM) in CH_3CN. Solutions were irradiated with a green LED. Right: Linear regressions for a decreasing of the absorbance at 410 nm for ***A***,***B*** and ***C***.

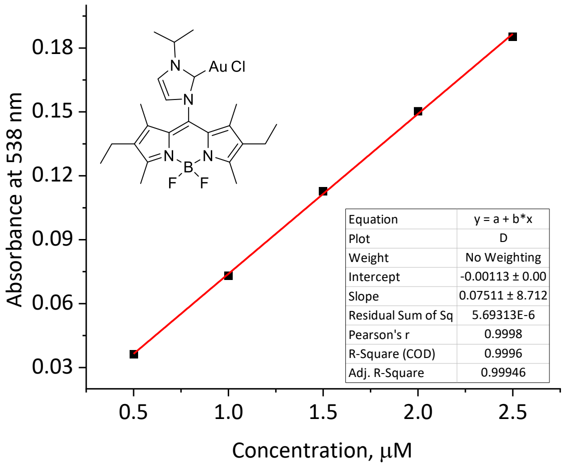

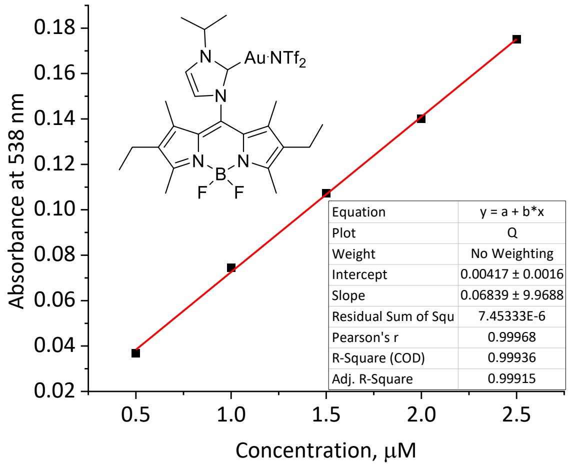

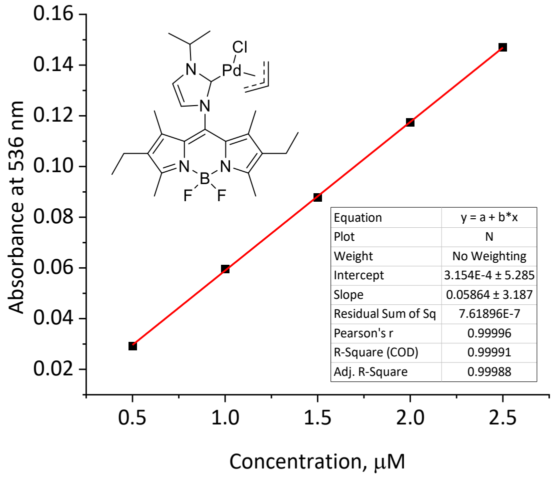

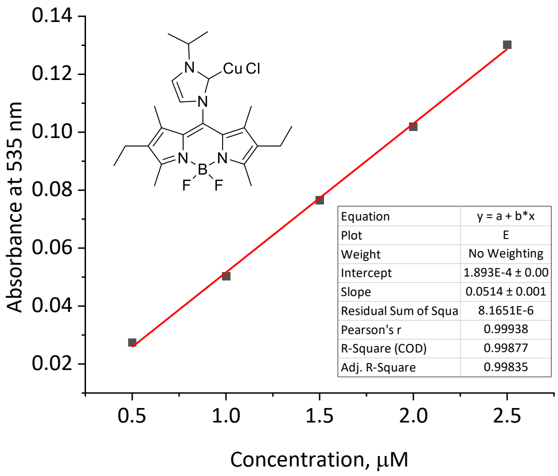

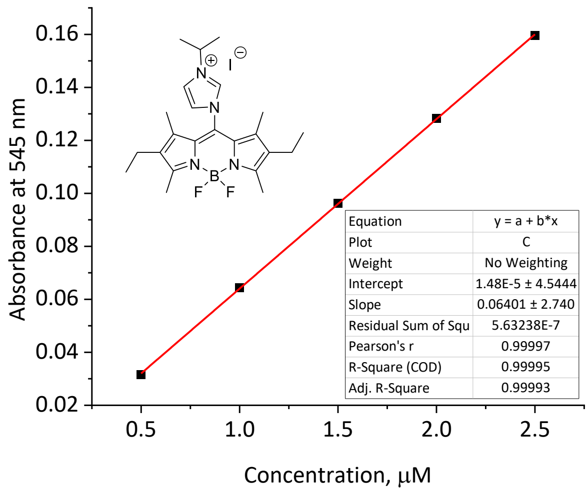

Figure S10. Absorbance at $\lambda_{abs, max}$ for the corresponding metal complexes with different concentrations in CH_3CN solution.

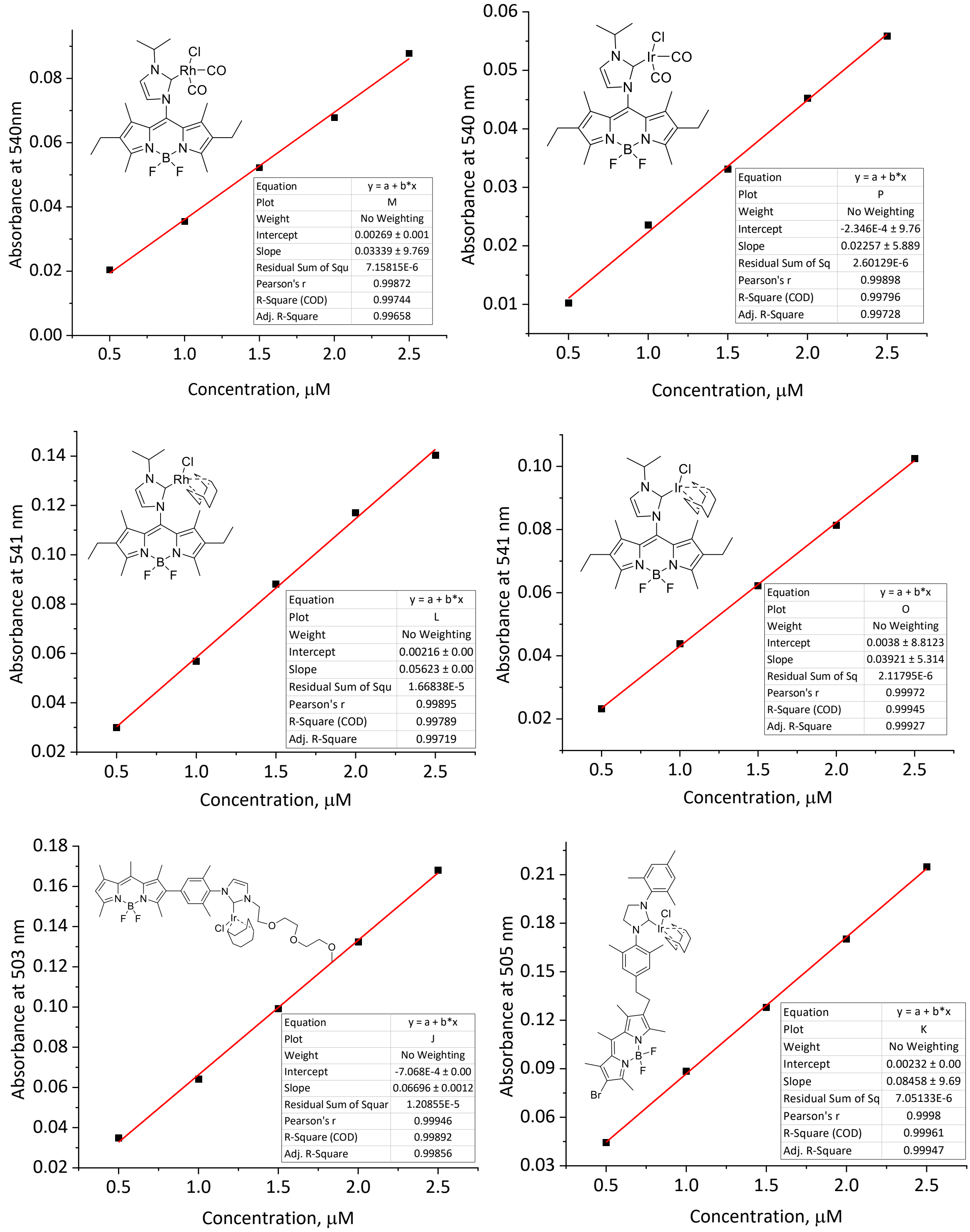

Figure S11. Absorbance at $\lambda_{abs,\ max}$ for the corresponding metal complexes with different concentrations in CH_3CN solution.

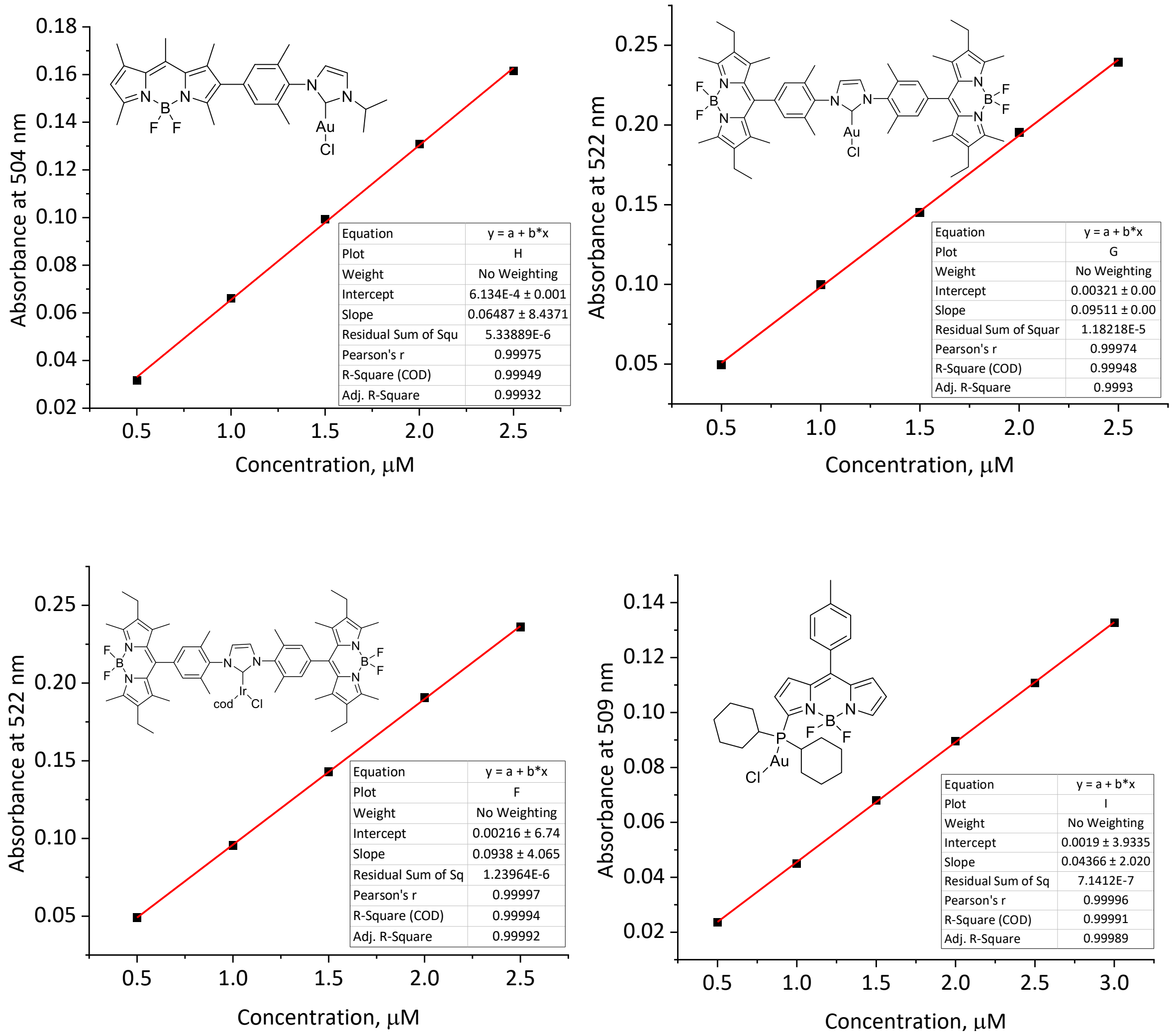

Figure S12. Absorbance at $\lambda_{abs, max}$ for the corresponding metal complexes with different concentrations in CH_3CN solution.

Fluorescence measurements

Quantum yields were determined according to the literature procedure (U. Resch-Genger, K. Rurack, *Pure Appl. Chem.*, **2013**, 85, 2005–2026) using rhodamine 6G (from Sigma-Aldrich, BioReagent, suitable for fluorescence) as the standard. Absorption and emission spectra for all compounds and standards were obtained over a range of concentrations (200 nM to 0.5 µM, in acetonitrile) where a linear correlation between concentration and absorption was observed. The absorbance was within the range of 0.01 to 0.12. The quantum yield was calculated according to the equation:

$$\varphi_x = \varphi_{st}(\frac{r_x}{r_{st}})(\frac{\eta_x}{\eta_{st}})^2$$

where the subscripts *st* and *x* denote standard and test respectively, φ_x is the fluorescence quantum yield, *r* the gradient from the plot of integrated fluorescence intensity vs. absorbance, and η the refractive index of the solvent. φ_{st} = 0.95 in EtOH.

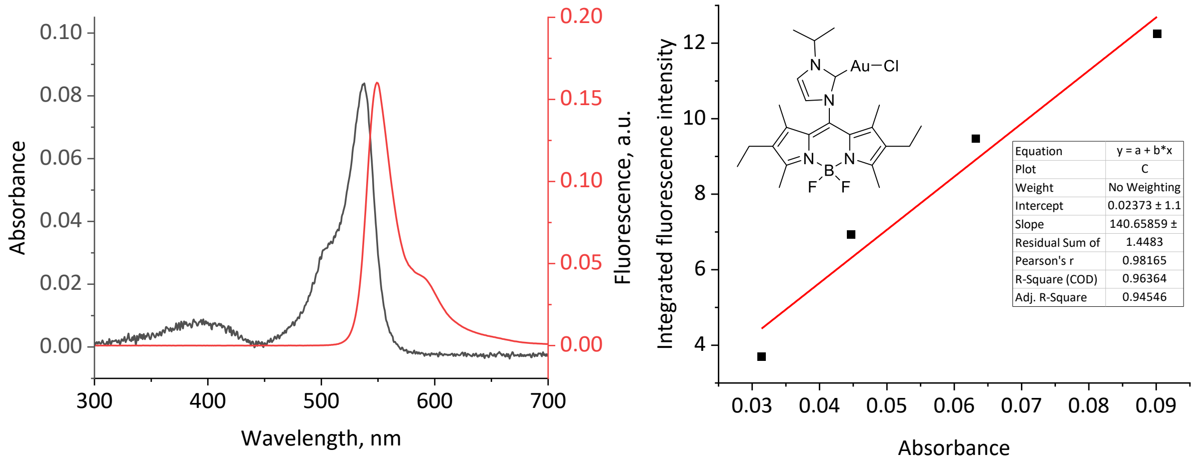

Figure S13. Left: absorbance (black) and emission (red, λ_{exc} = 540 nm) spectra of [AuCl(**3**)] in CH_3CN solution. Right: integrated fluorescence intensity *vs.* absorbance plot for [AuCl(**3**)].

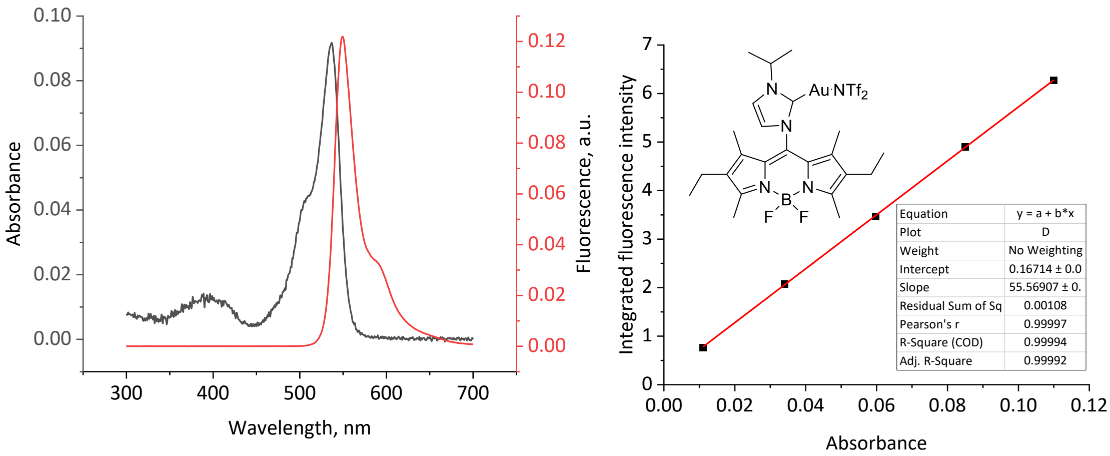

Figure S14. Left: absorbance (black) and emission (red, λ_{exc} = 540 nm) spectra of [$AuNTf_2$(**3**)] in CH_3CN solution. Right: integrated fluorescence intensity *vs.* absorbance plot for [$AuNTf_2$(**3**)].

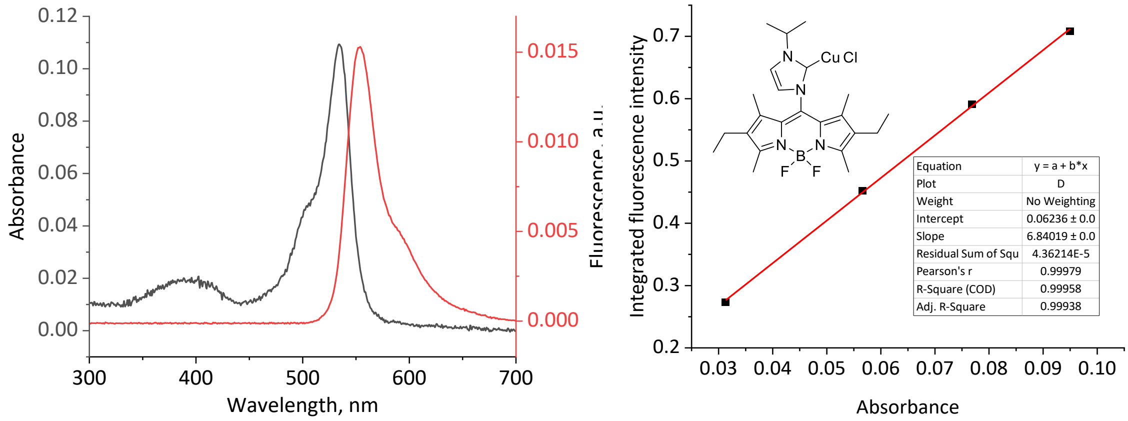

Figure S15. Left: absorbance (black) and emission (red, λ_{exc} = 540 nm) spectra of [CuCl(**3**)] in CH_3CN solution. Right: integrated fluorescence intensity *vs.* absorbance plot for [CuCl(**3**)].

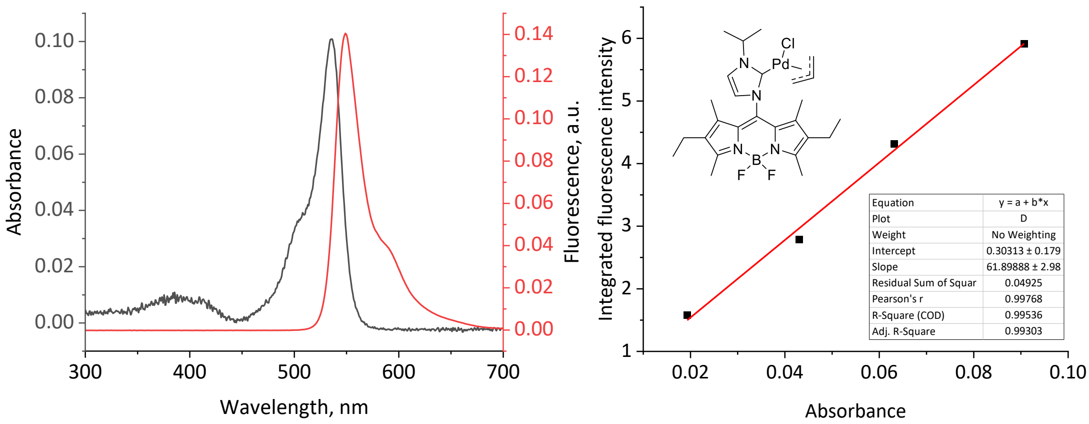

Figure S16. Left: absorbance (black) and emission (red, λ_{exc} = 540 nm) spectra of [PdCl(ally)(**3**)] in CH_3CN solution. Right: integrated fluorescence intensity *vs.* absorbance plot for [PdCl(allyl)(**3**)].

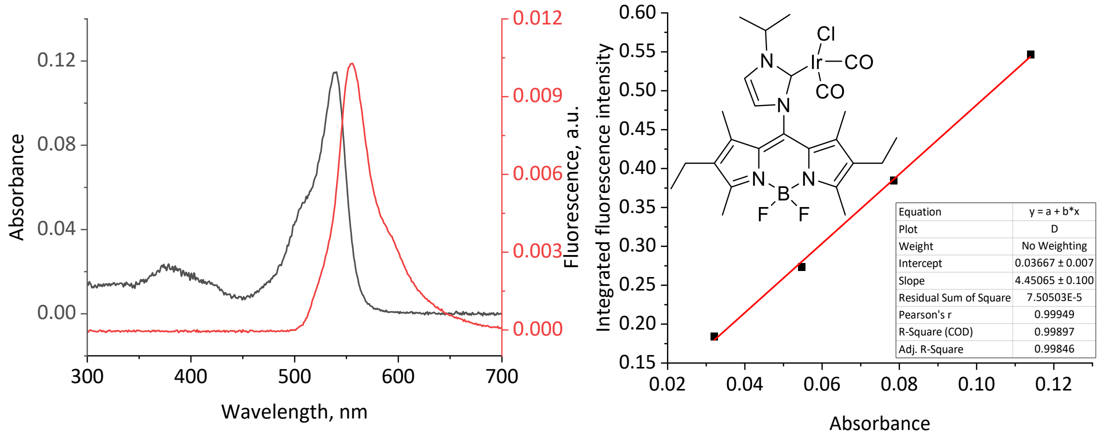

Figure S17. Left: absorbance (black) and emission (red, λ_{exc} = 540 nm) spectra of [IrCl(CO)$_2$(**3**)] in CH_3CN solution. Right: integrated fluorescence intensity *vs.* absorbance plot for [IrCl(CO)$_2$(**3**)].

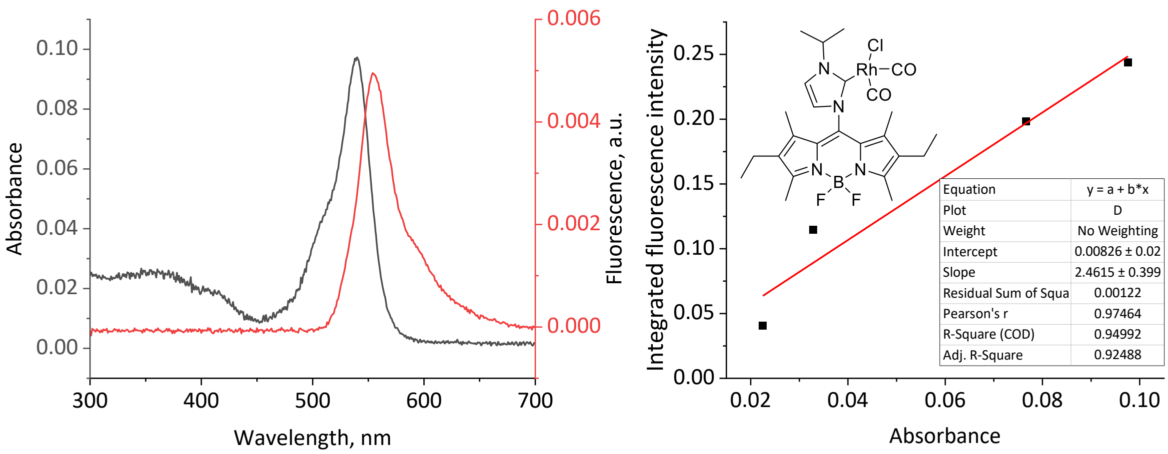

Figure S18. Left: absorbance (black) and emission (red, λ_{exc} = 540 nm) spectra of [RhCl(CO)$_2$(**3**)] in CH_3CN solution. Right: integrated fluorescence intensity *vs.* absorbance plot for [RhCl(CO)$_2$(**3**)].

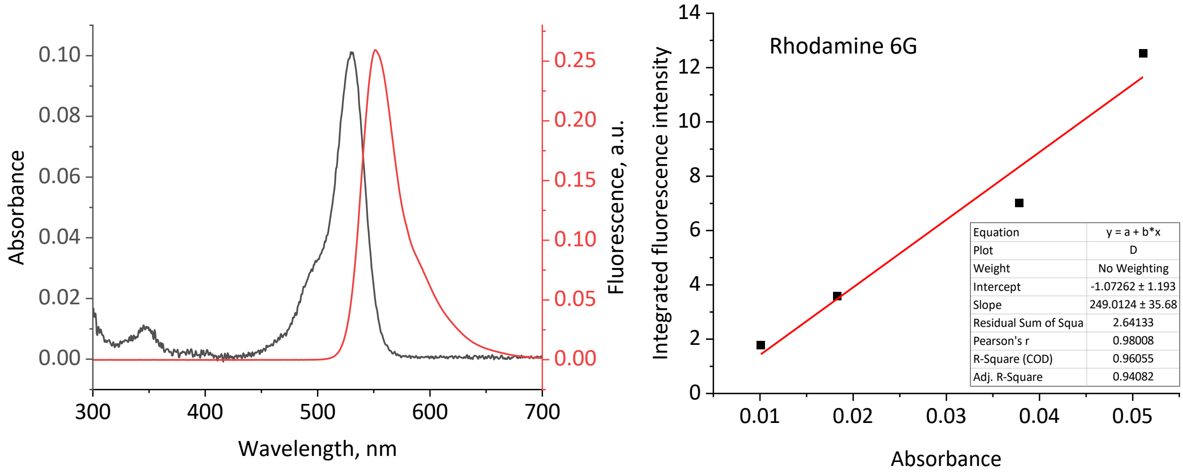

Figure S19. Left: absorbance (black) and emission (red, λ_{exc} = 540 nm) spectra of Rhodamine 6G in EtOH solution. Right: integrated fluorescence intensity *vs.* absorbance plot for Rhodamine 6G.

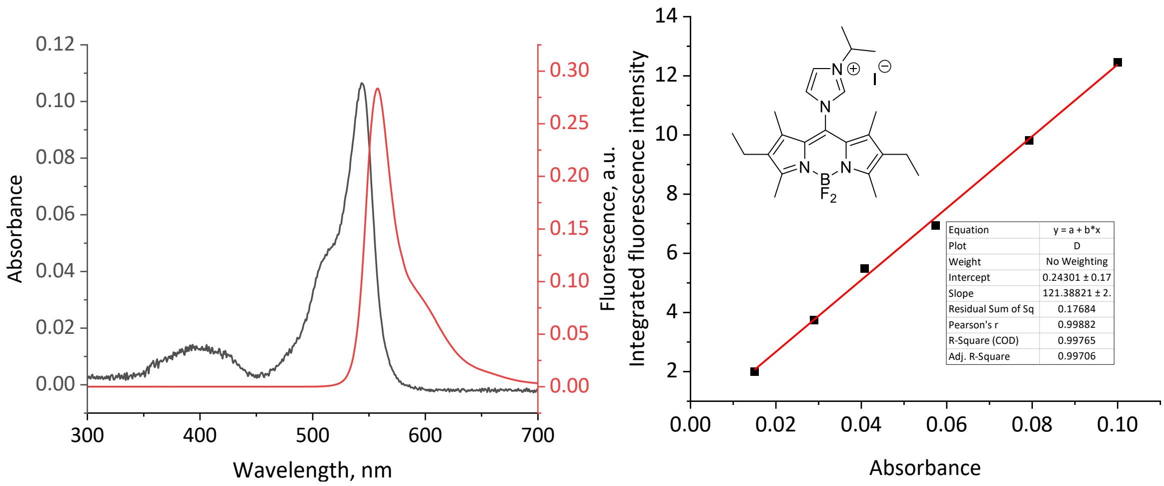

Figure S20. Left: absorbance (black) and emission (red , λ_{exc} = 540 nm) spectra of **3**·HI in CH_3CN solution. Right: integrated fluorescence intensity *vs.* absorbance plot for BODIPY HI **3**.

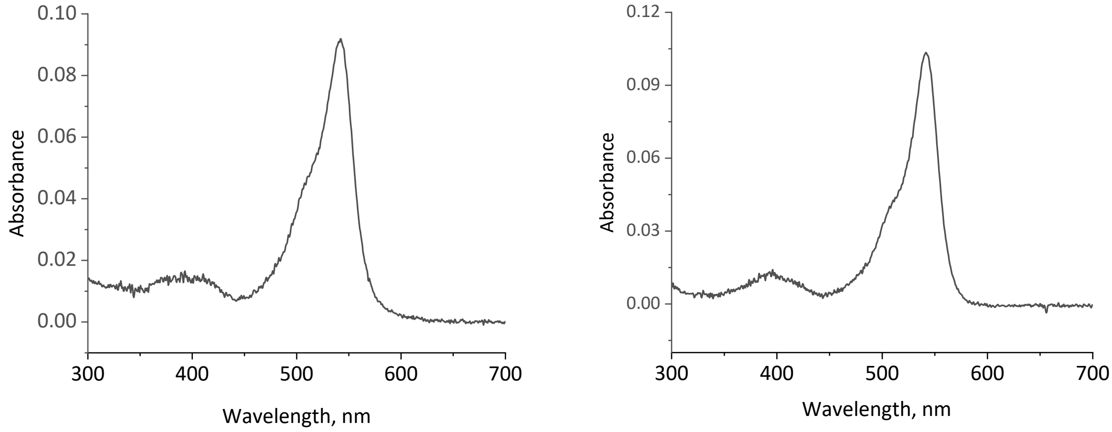

Figure S21. Left: absorbance spectra of [IrCl(cod)(**3**)] in CH_3CN solution. Right: absorbance spectra of [RhCl(cod)(**3**)] in CH_3CN solution.

NMR spectra

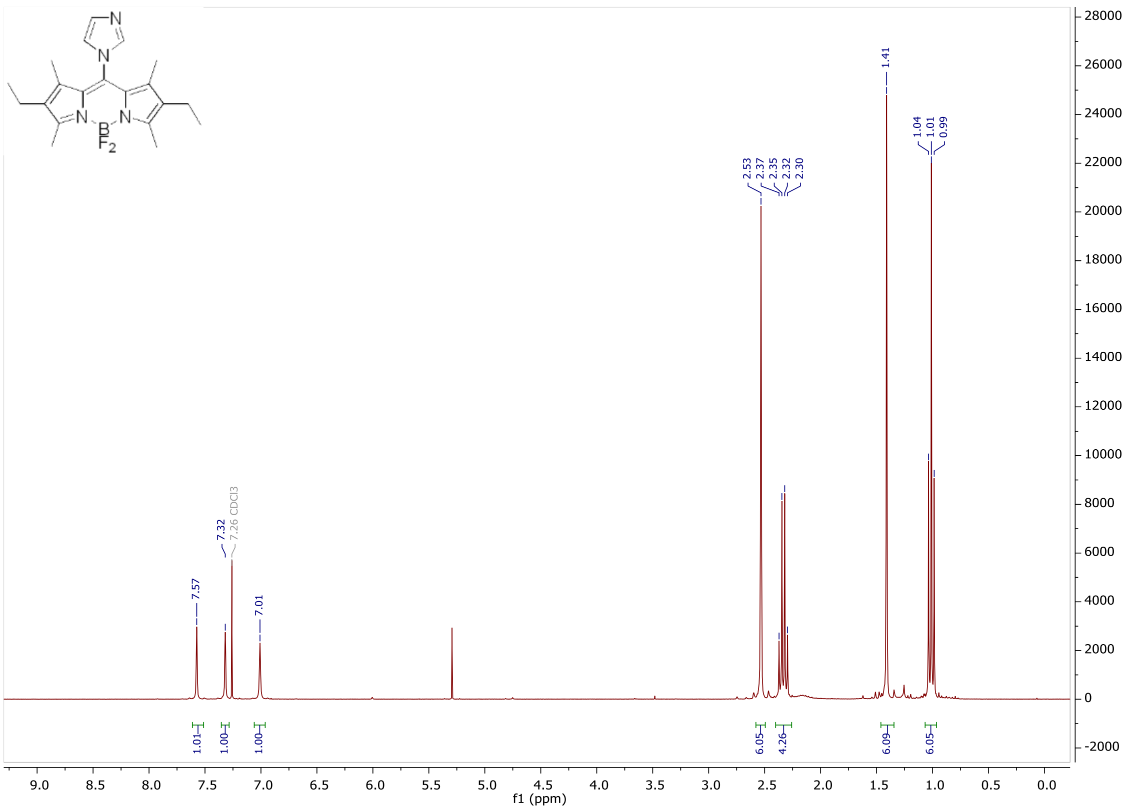

Figure S22. ^{1}H-NMR (300 MHz) of 8-imidazolo-BODIPY **2** in $CDCl_3$.

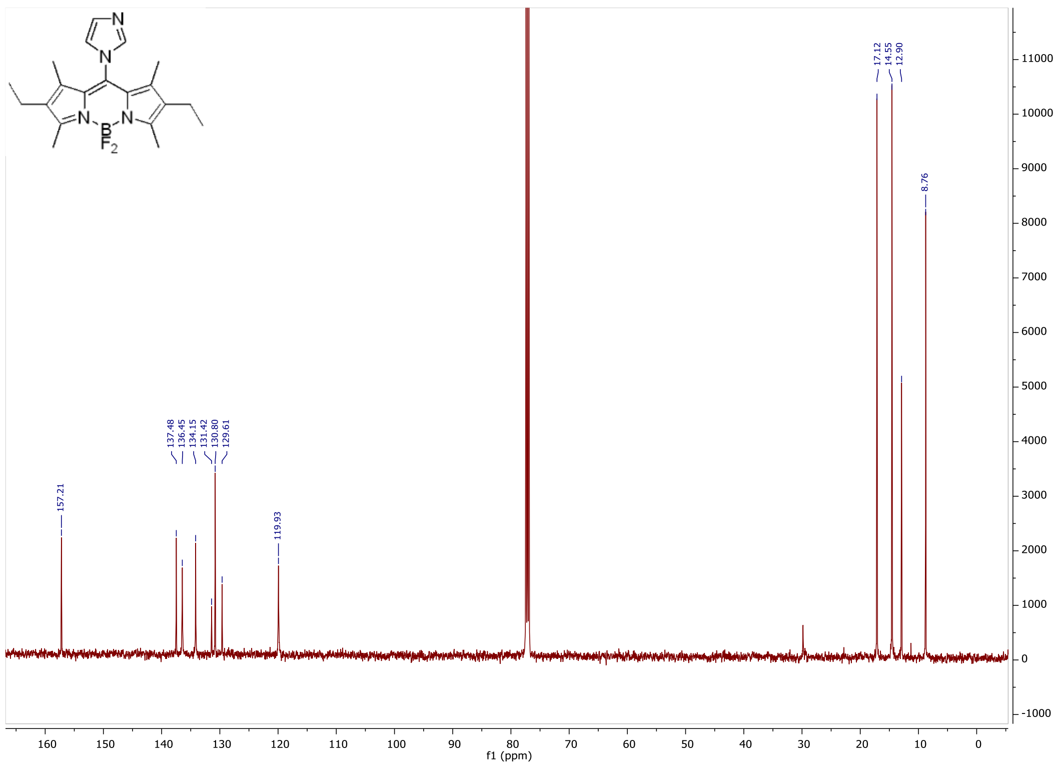

Figure S23. $^{13}C\{^{1}H\}$-NMR (126 MHz) of 8-imidazolo-BODIPY **2** in $CDCl_3$.

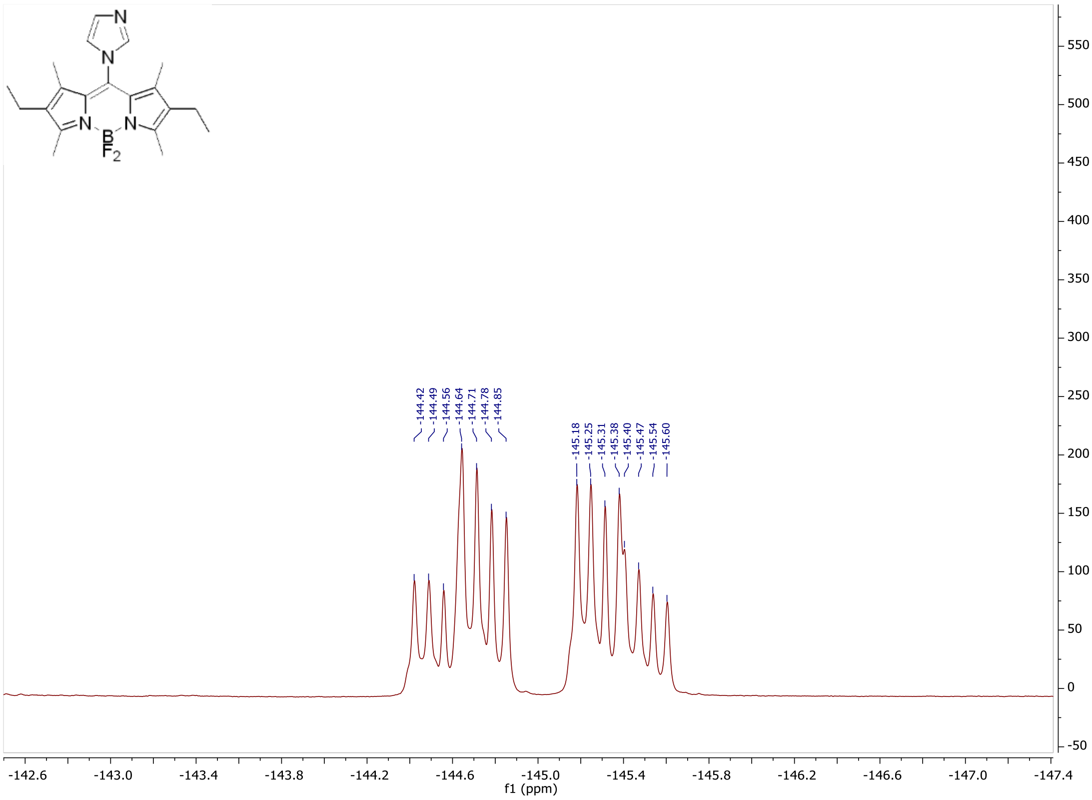

Figure S24. ^{19}F-NMR (471 MHz) of 8-imidazolo-BODIPY **2** in $CDCl_3$.

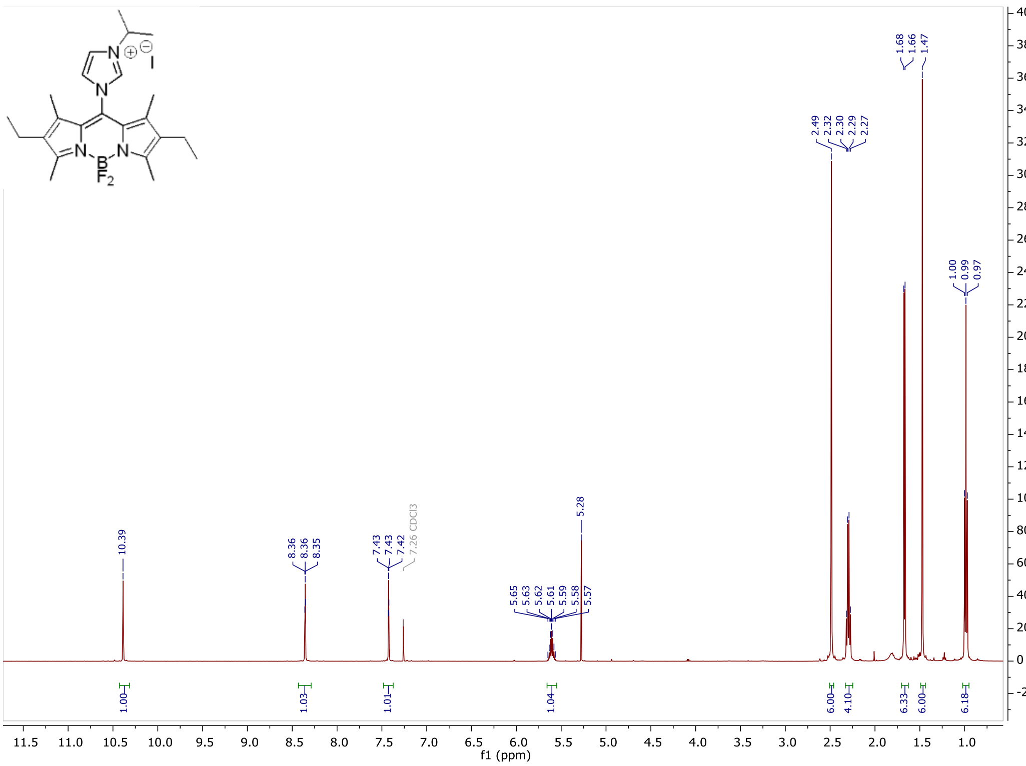

Figure S25. ^{1}H-NMR (500 MHz) of BODIPY imidazolium salt **3** in $CDCl_3$.

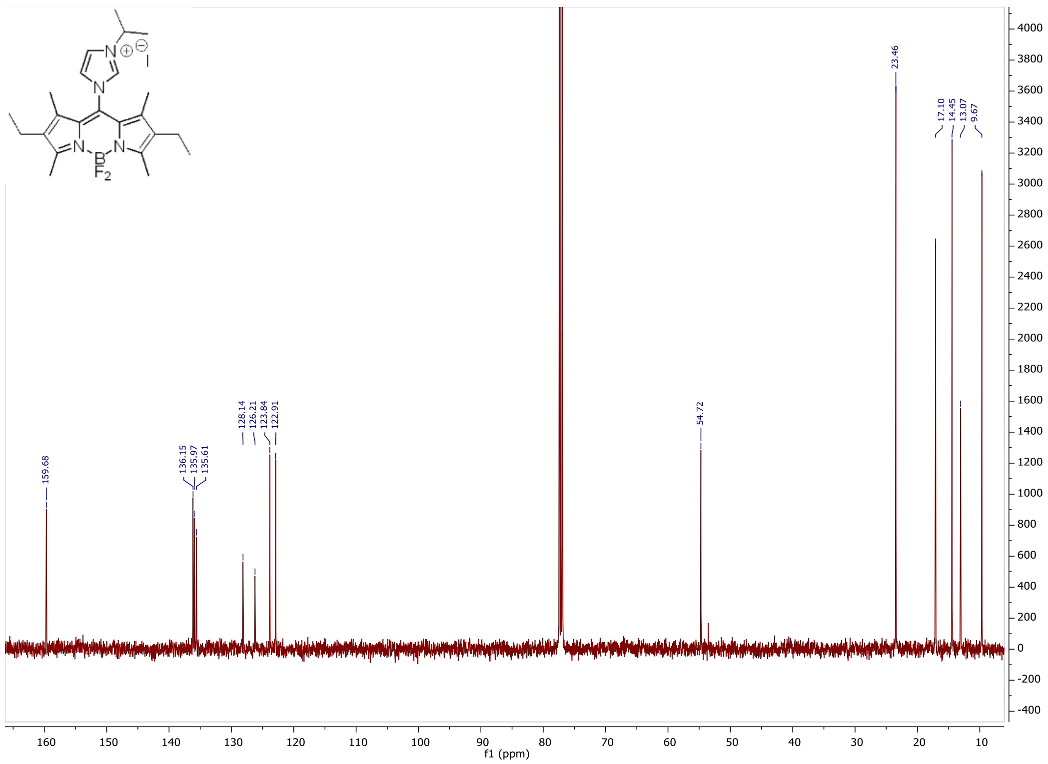

Figure S26. $^{13}C\{^{1}H\}$-NMR (126 MHz) of BODIPY imidazolium salt **3** in $CDCl_3$.

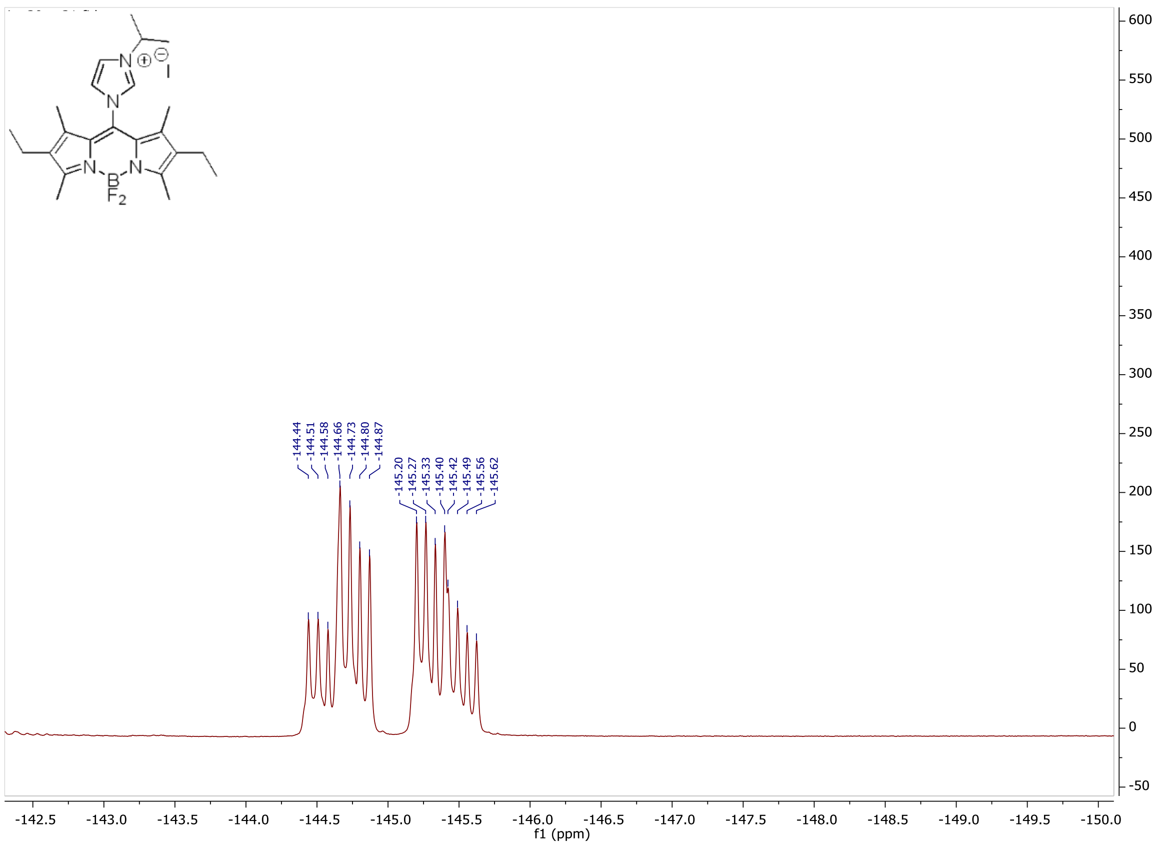

Figure S27. ^{19}F-NMR (471 MHz) of BODIPY imidazolium salt **3** in $CDCl_3$.

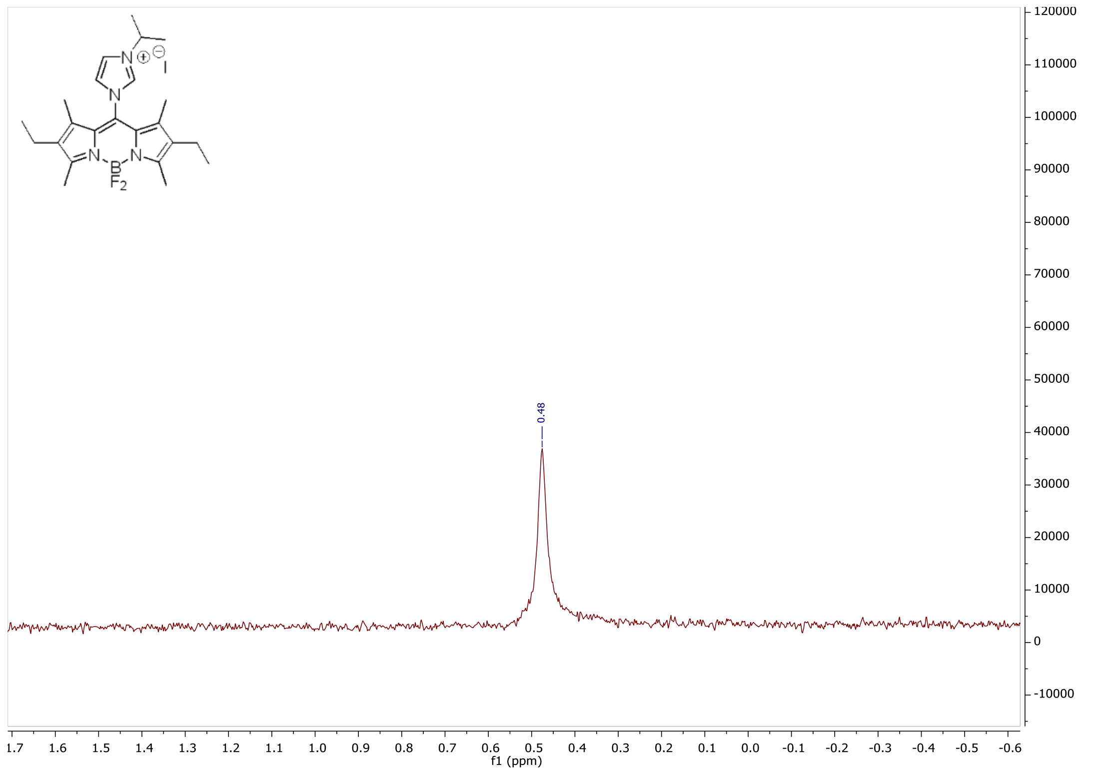

Figure S28. ^{11}B-NMR (160 MHz) of BODIPY imidazolium salt **3** in $CDCl_3$.

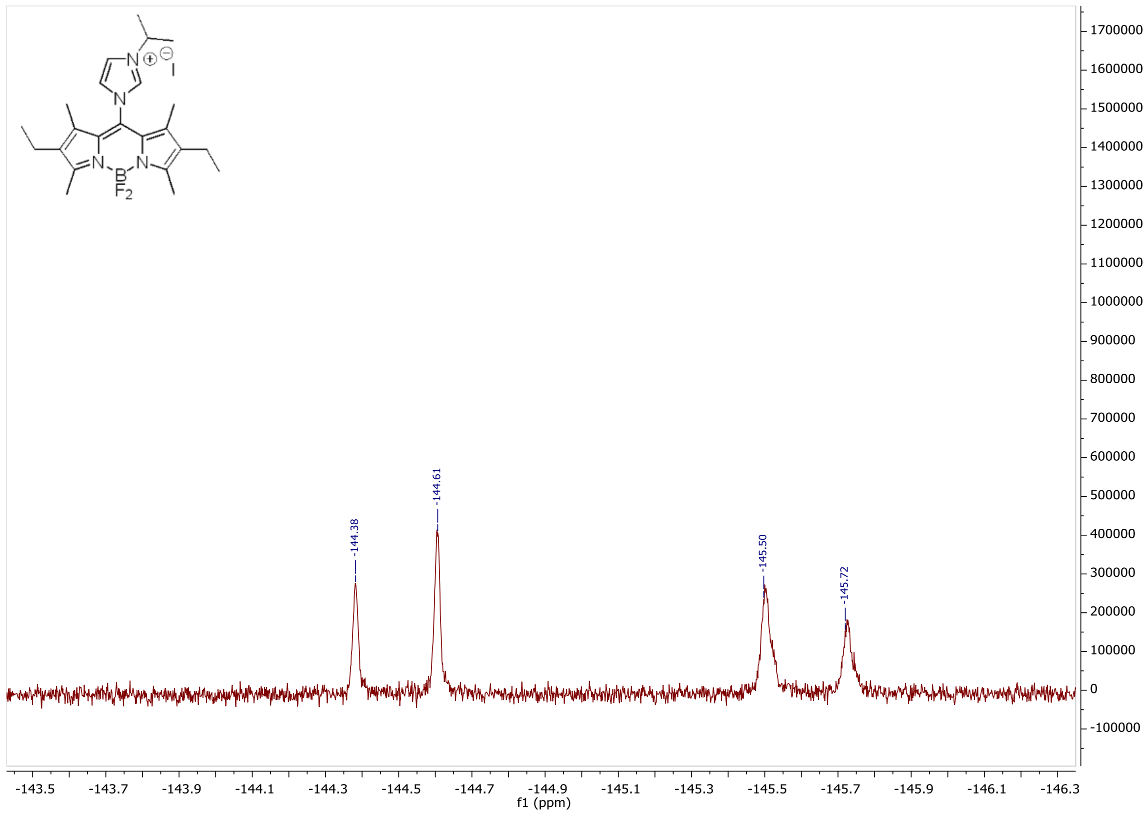

Figure S29. ^{19}F{^{11}B}-NMR (471 MHz) of BODIPY imidazolium salt **3** in $CDCl_3$.

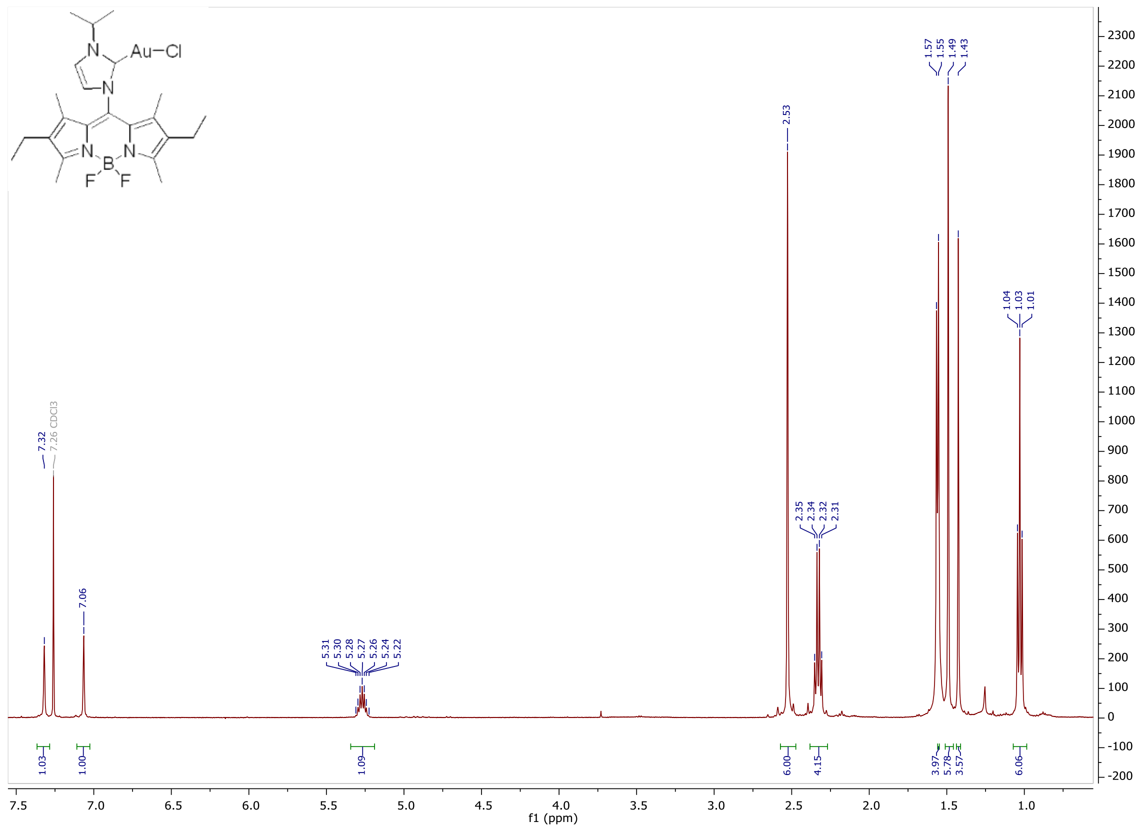

Figure S30. ^{1}H-NMR (500 MHz) of [AuCl(**3**)] complex in $CDCl_3$.

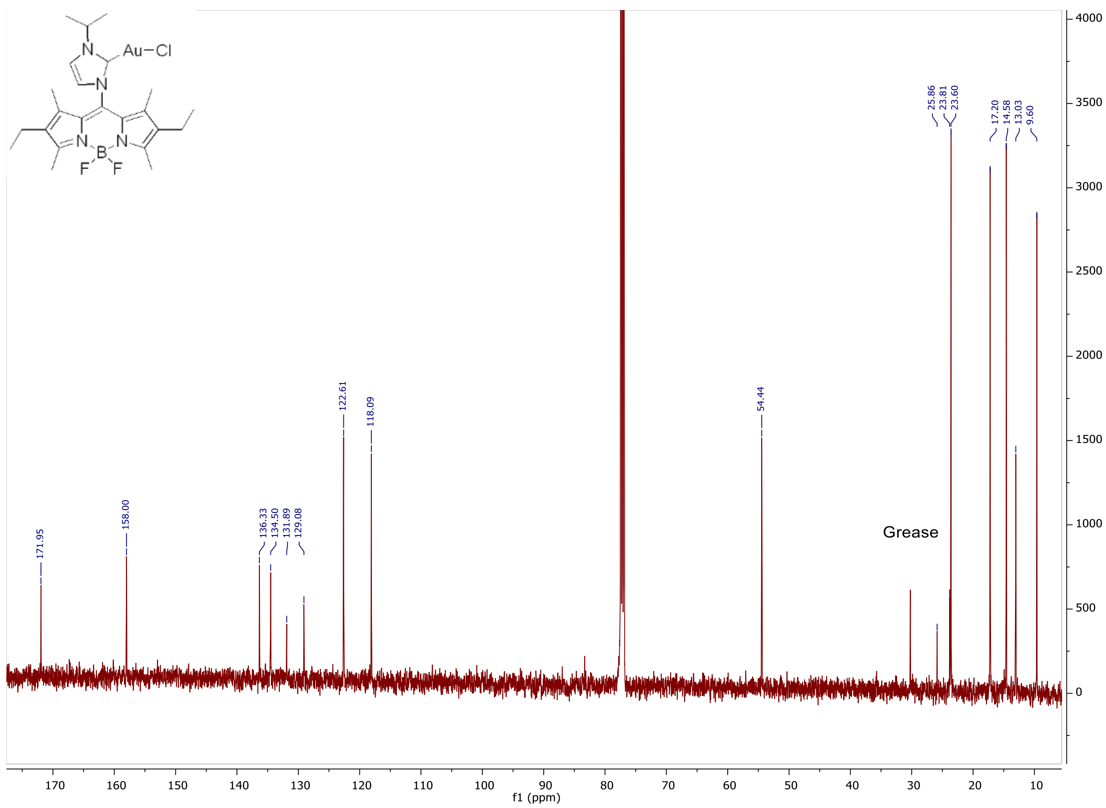

Figure S31. ^{13}C{^{1}H}-NMR (126 MHz) of [AuCl(**3**)] complex in $CDCl_3$.

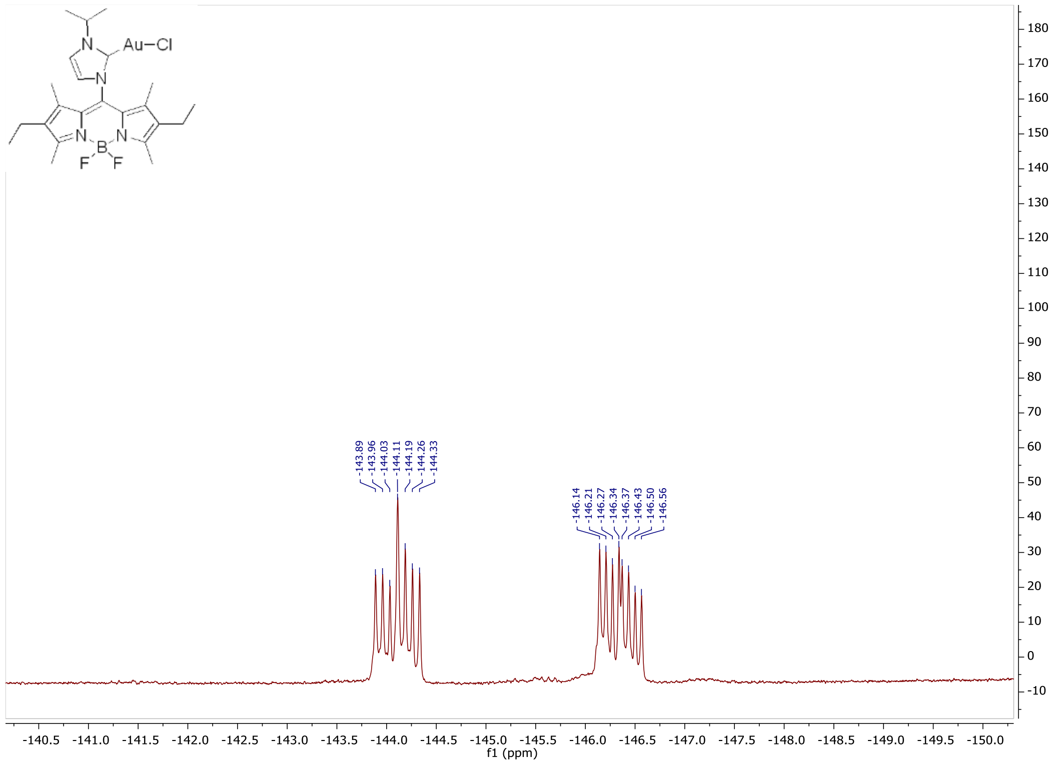

Figure S32. ^{19}F-NMR (471 MHz) of [AuCl(**3**)] complex in $CDCl_3$.

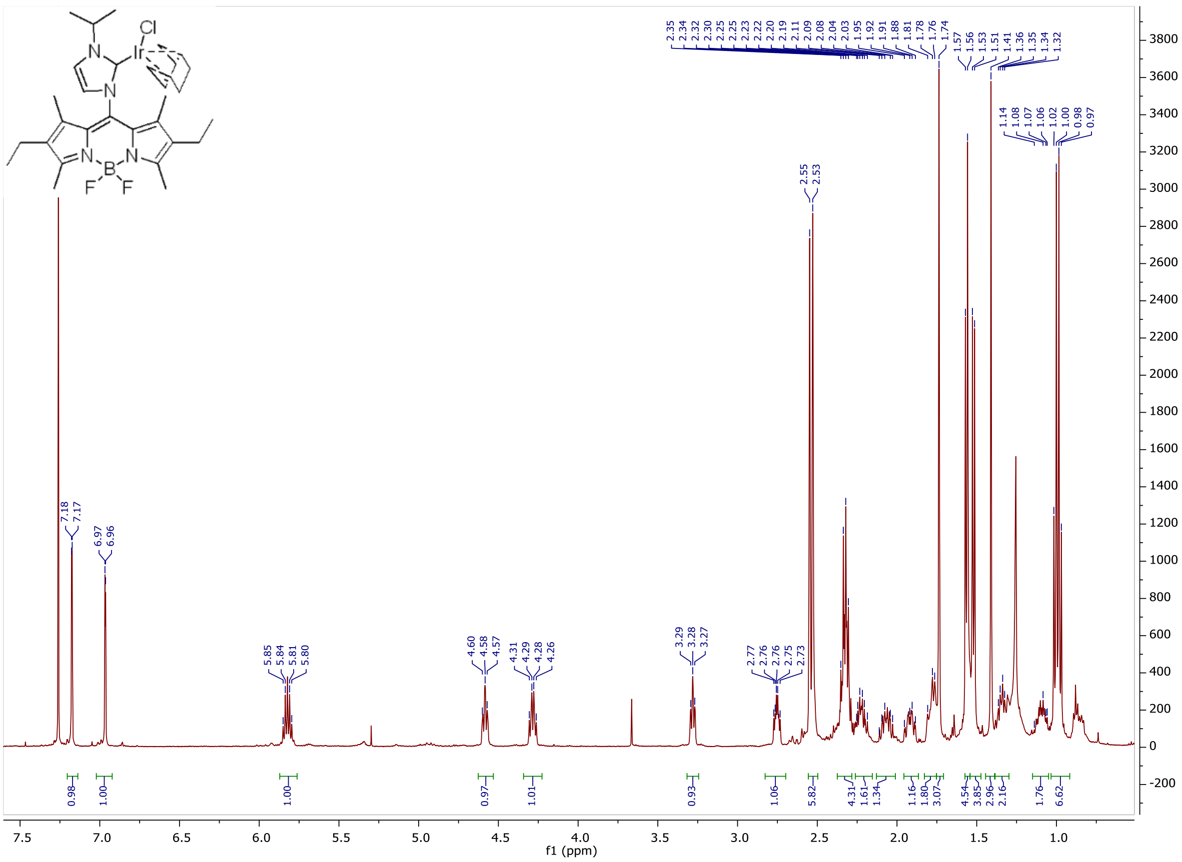

Figure S33. ^{1}H-NMR (500 MHz) of [IrCl(cod)(**3**)] complex in $CDCl_3$.

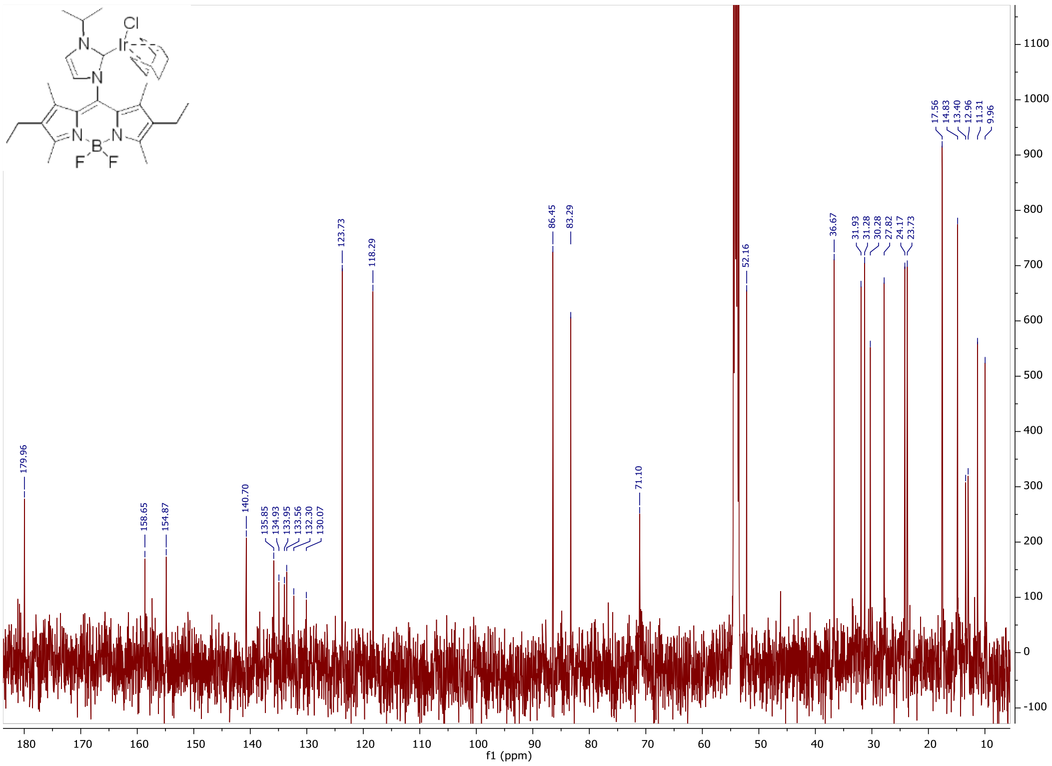

Figure S34. $^{13}C\{^{1}H\}$-NMR (126 MHz) of [IrCl(cod)(**3**)] complex in CD_2Cl_2.

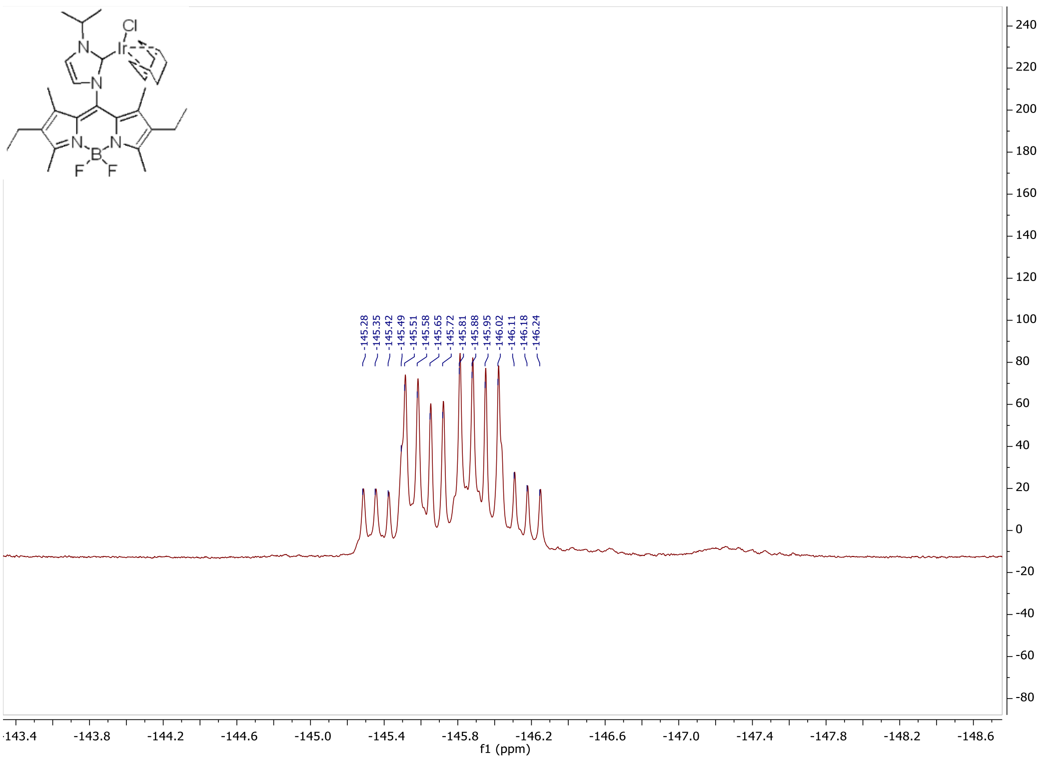

Figure S35. ^{19}F-NMR (471 MHz) of [IrCl(cod)(**3**)] complex in CD_2Cl_2.

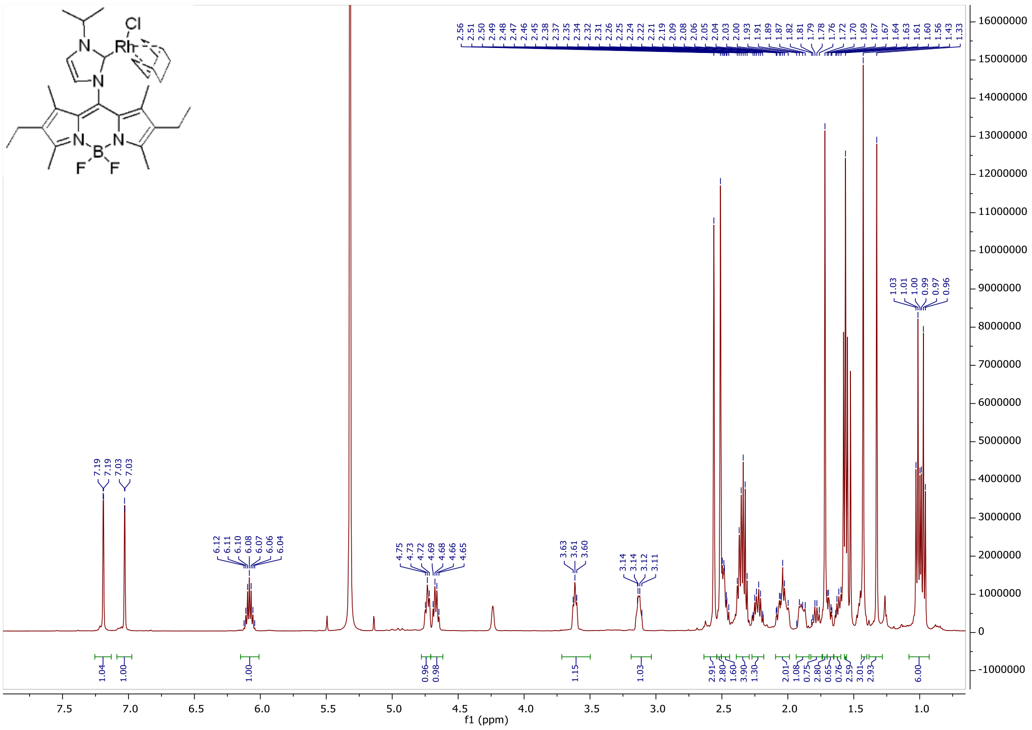

Figure S36. ^{1}H-NMR (500 MHz) of [RhCl(cod)(**3**)] complex in CD_2Cl_2.

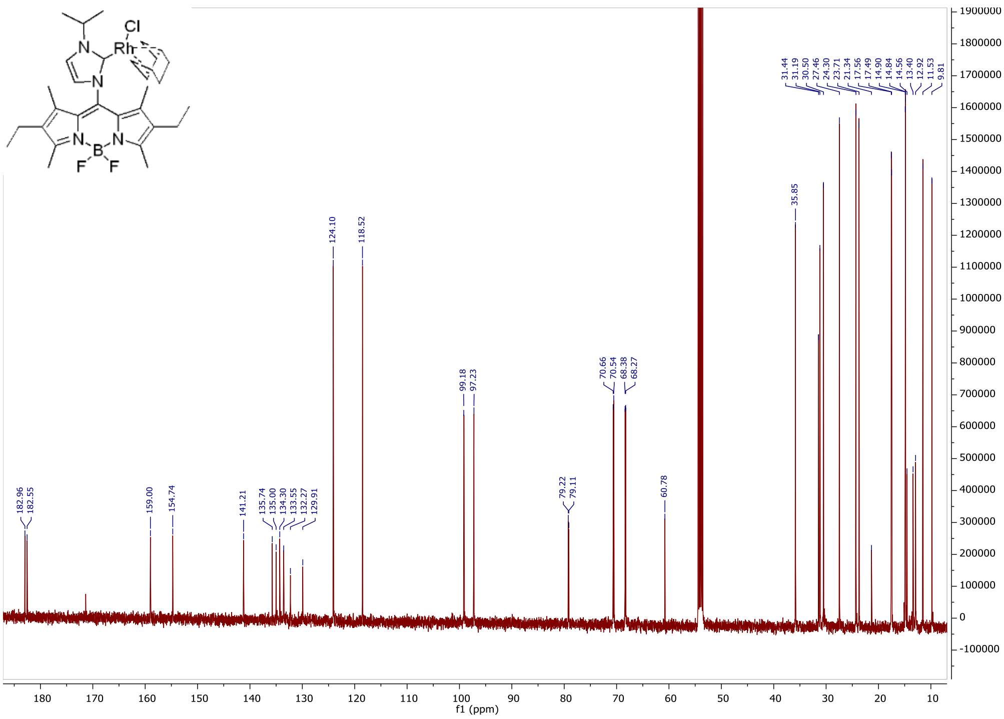

Figure S37. $^{13}C\{^{1}H\}$-NMR (126 MHz) of [RhCl(cod)(**3**)] complex in CD_2Cl_2.

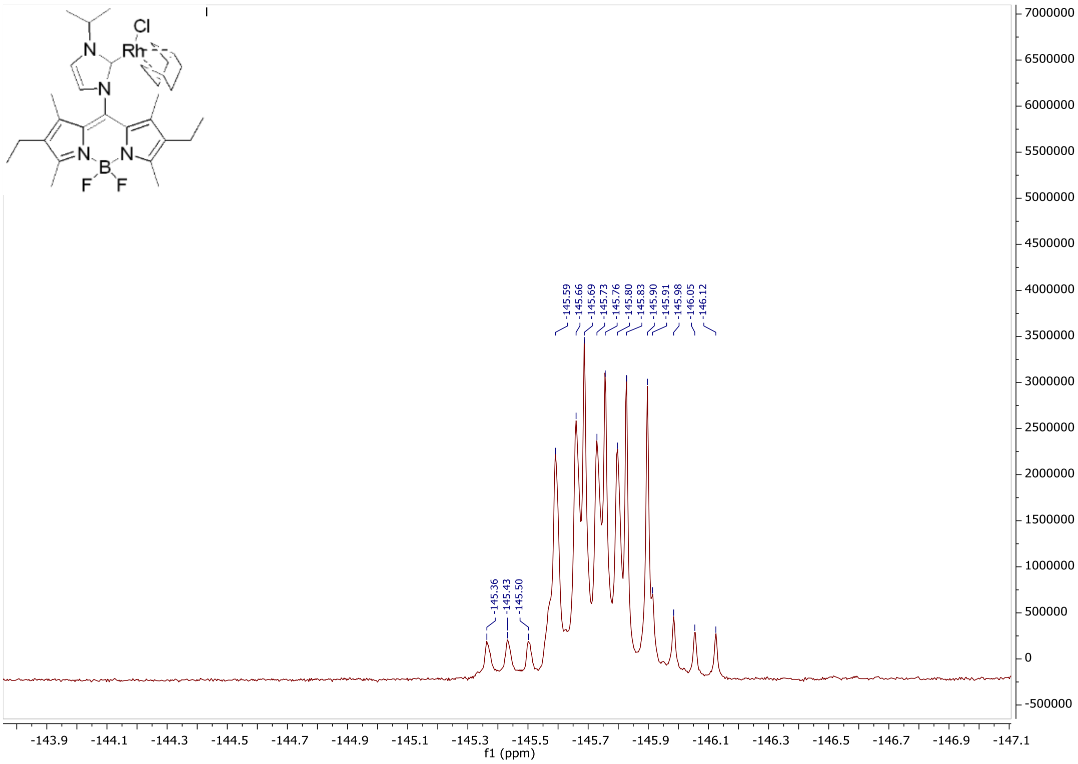

Figure S38. ^{19}F-NMR (471 MHz) of [RhCl(cod)(**3**)] complex in CD_2Cl_2.

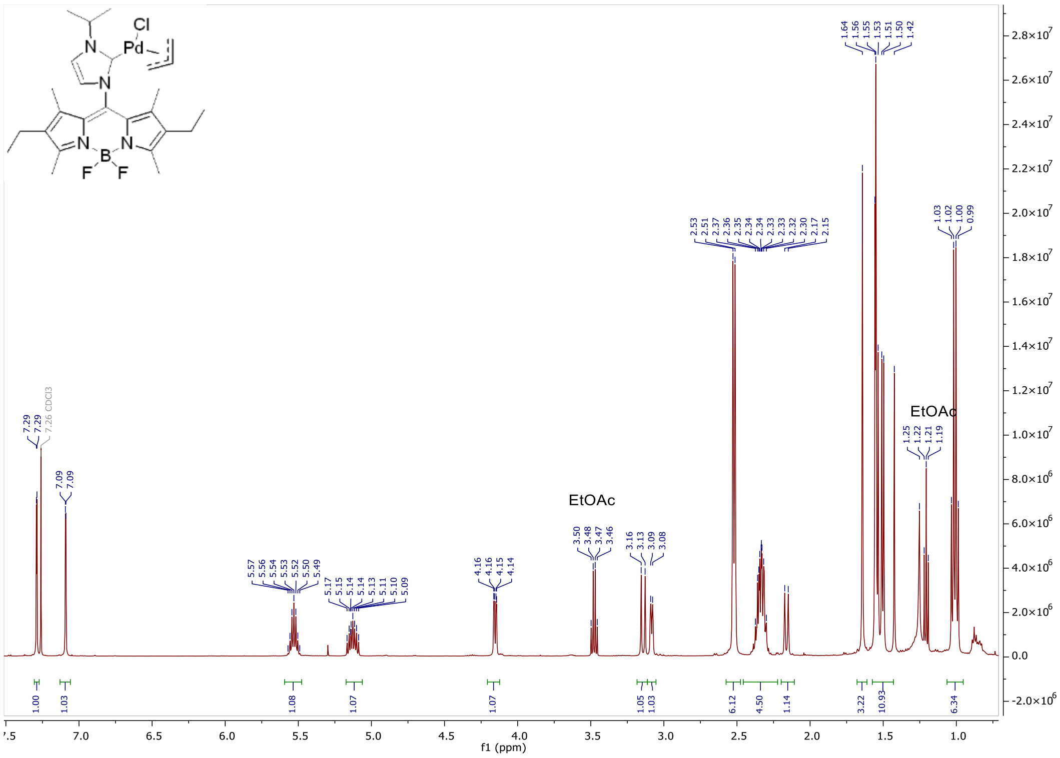

Figure S39. ^{1}H-NMR (500 MHz) of [PdCl(allyl)(**3**)] complex in $CDCl_3$.

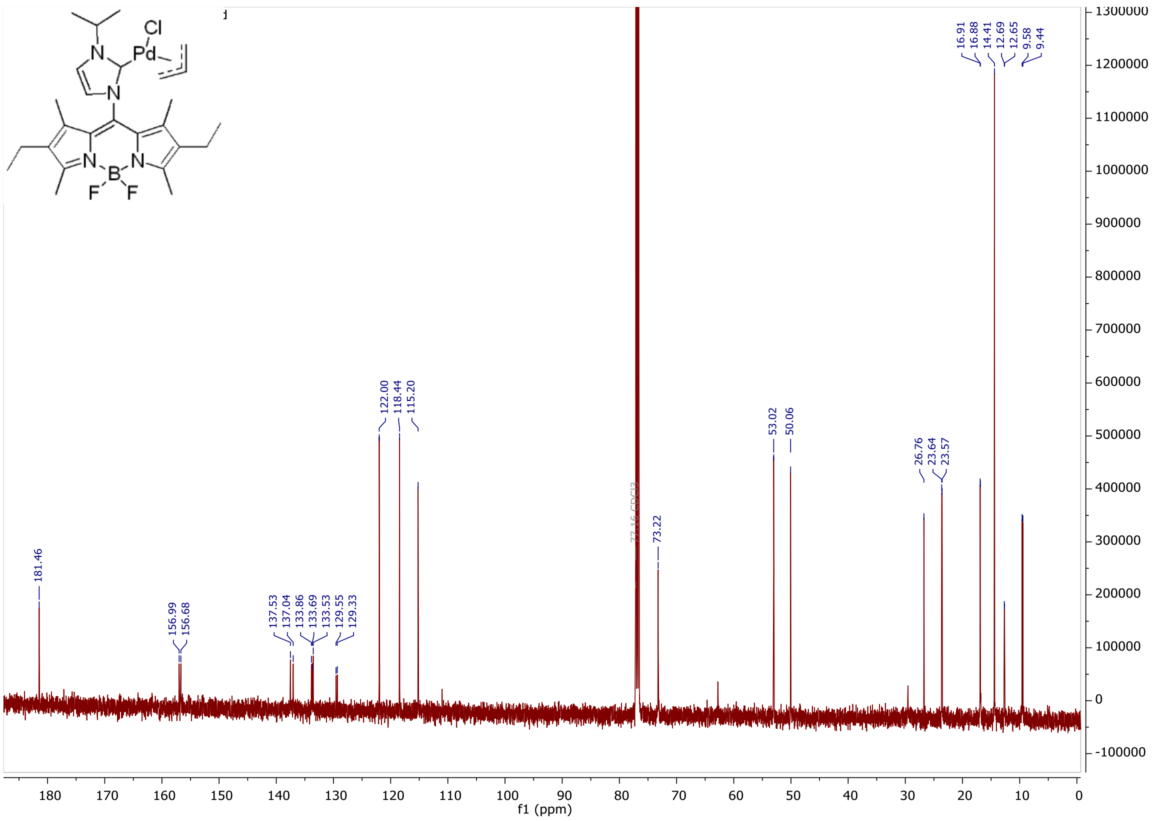

Figure S40. $^{13}C\{^{1}H\}$-NMR (126 MHz) of [PdCl(allyl)(**3**)] complex in $CDCl_3$.

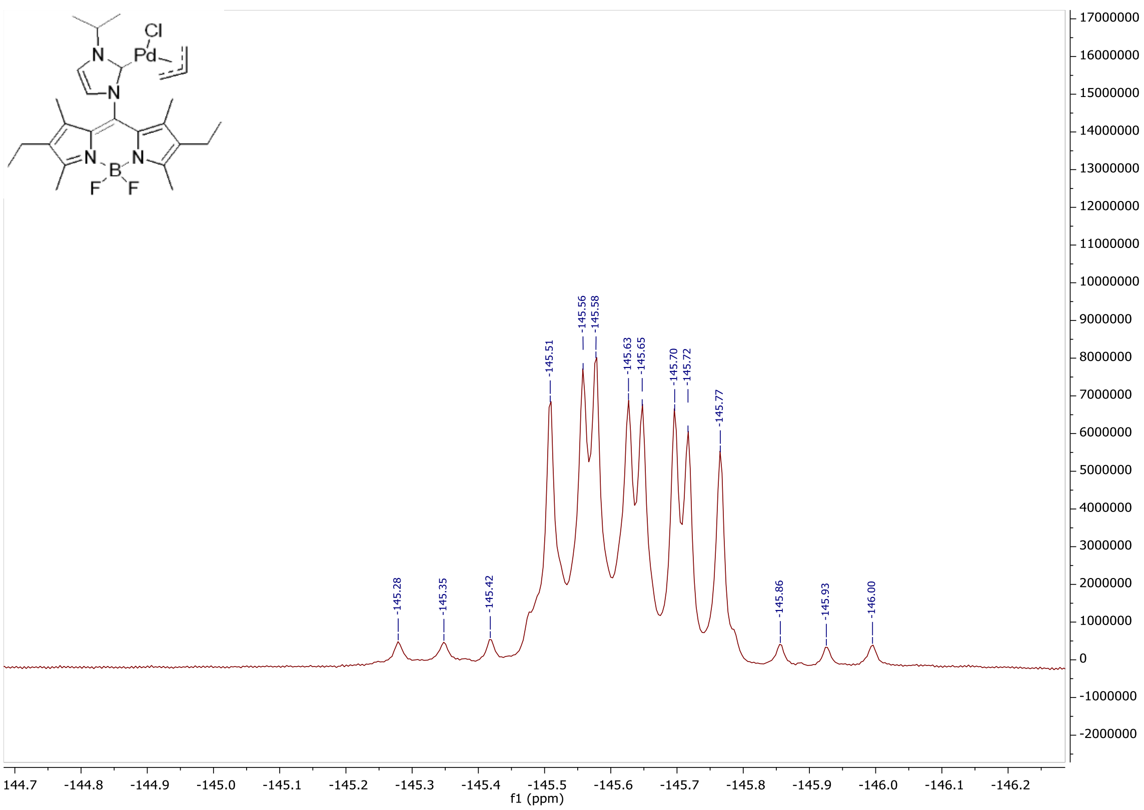

Figure S41. ^{19}F-NMR (471 MHz) of [PdCl(allyl)(**3**)] complex in $CDCl_3$.

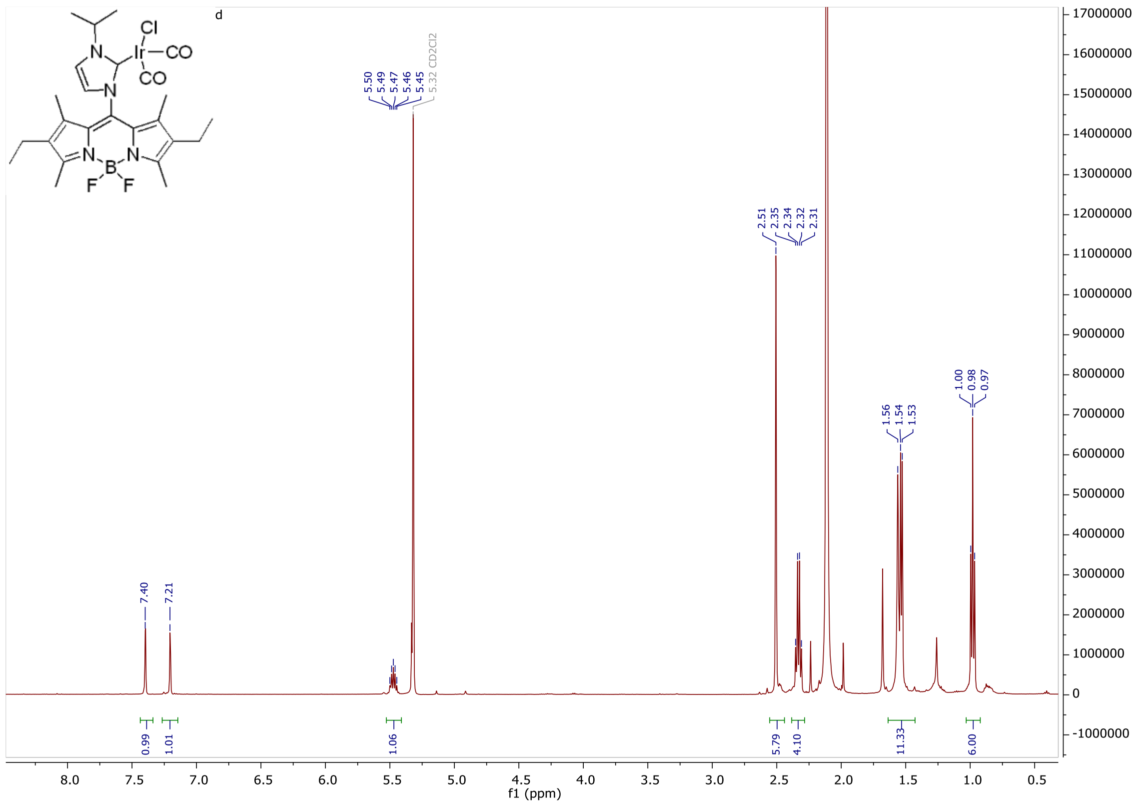

Figure S42. ^{1}H-NMR (500 MHz) of $[IrCl(CO)_2(\mathbf{3})]$ complex in CD_2Cl_2.

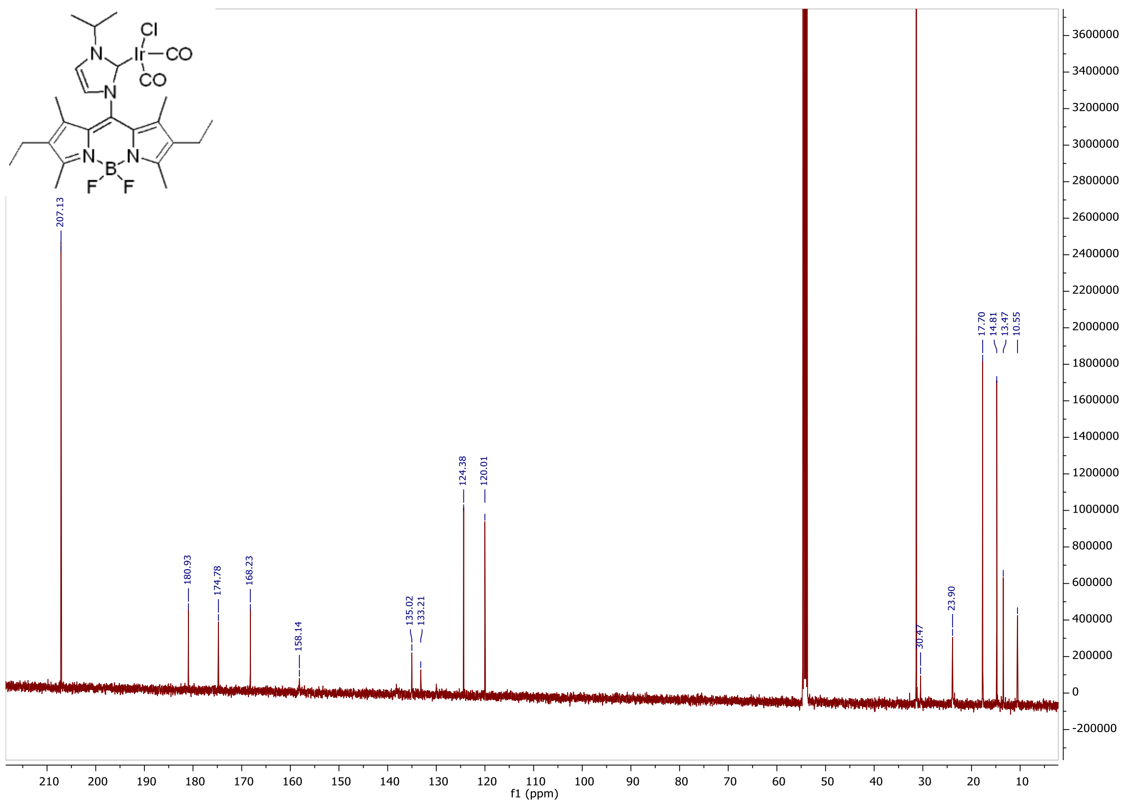

Figure S43. $^{13}C\{^{1}H\}$-NMR (126 MHz) of $[IrCl(CO)_2(\mathbf{3})]$ complex in CD_2Cl_2.

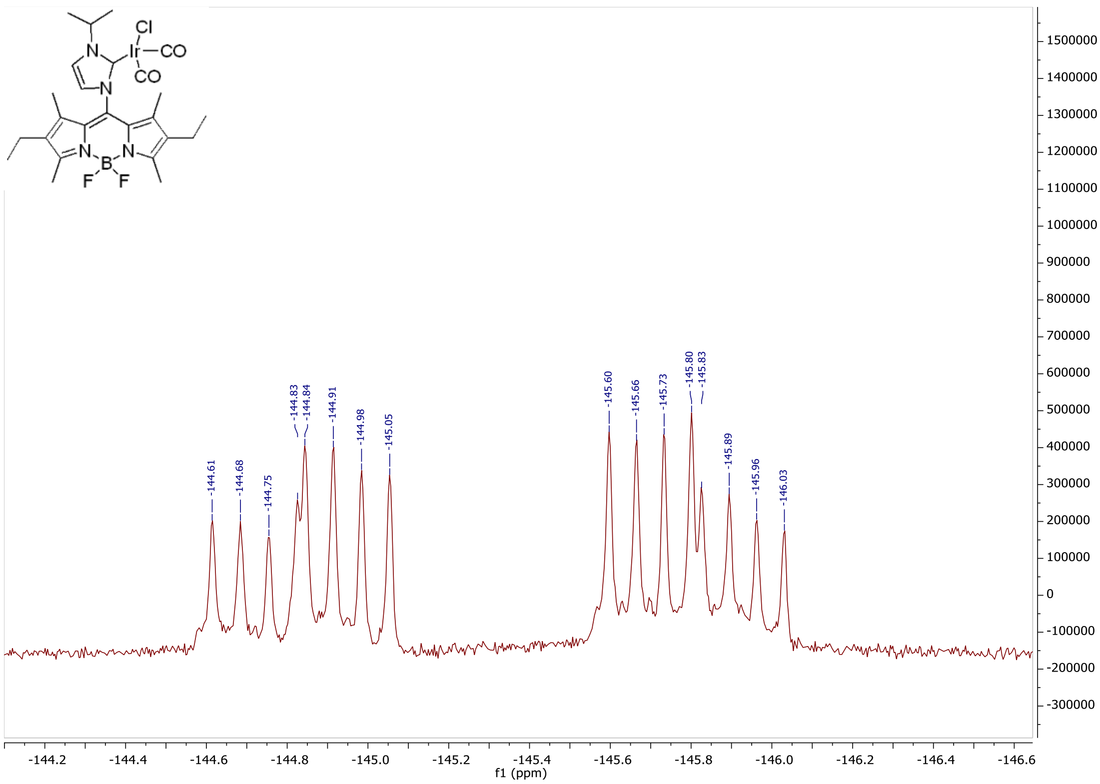

Figure S44. ^{19}F-NMR (471 MHz) of $[IrCl(CO)_2(\mathbf{3})]$ complex in CD_2Cl_2.

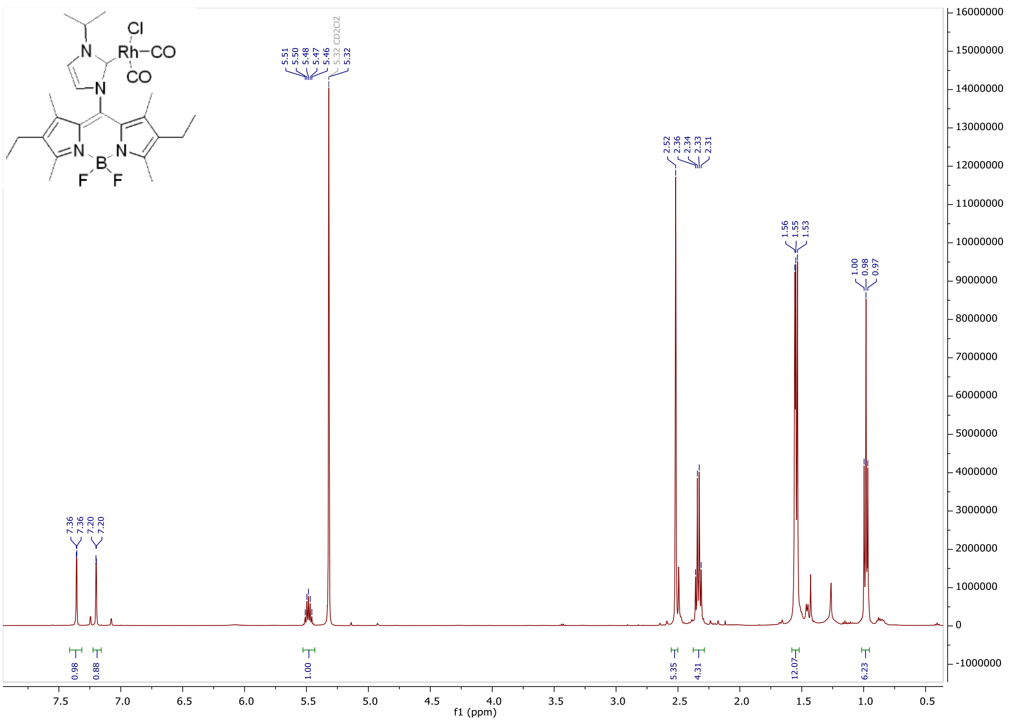

Figure S45. ^{1}H-NMR (500 MHz) of $[RhCl(CO)_2(\mathbf{3})]$ complex in CD_2Cl_2.

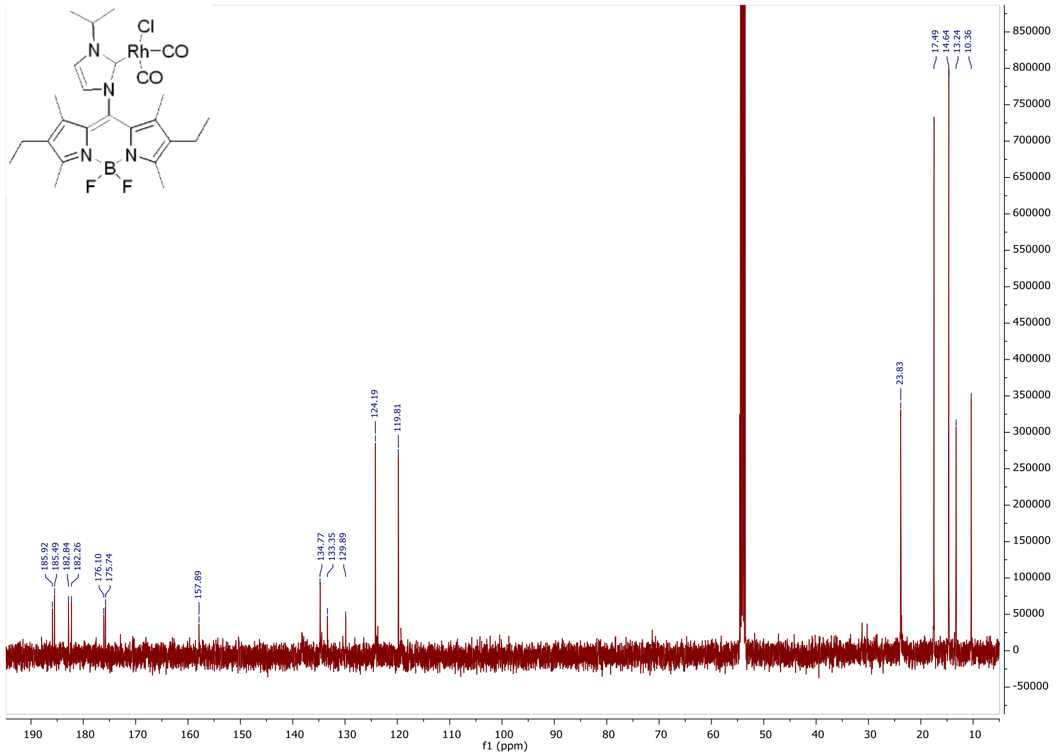

Figure S46. $^{13}C\{^{1}H\}$-NMR (126 MHz) of [RhCl(CO)$_2$(**3**)] complex in CD_2Cl_2.

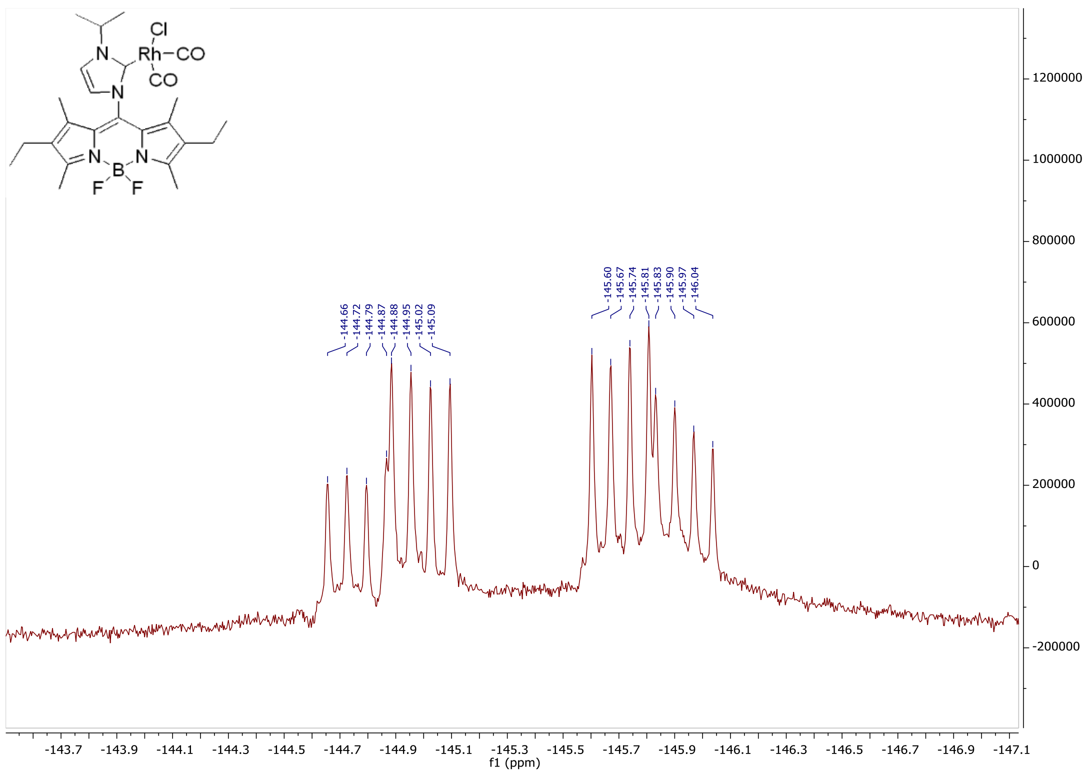

Figure S47. ^{19}F-NMR (471 MHz) of [RhCl(CO)$_2$(**3**)] complex in CD_2Cl_2.

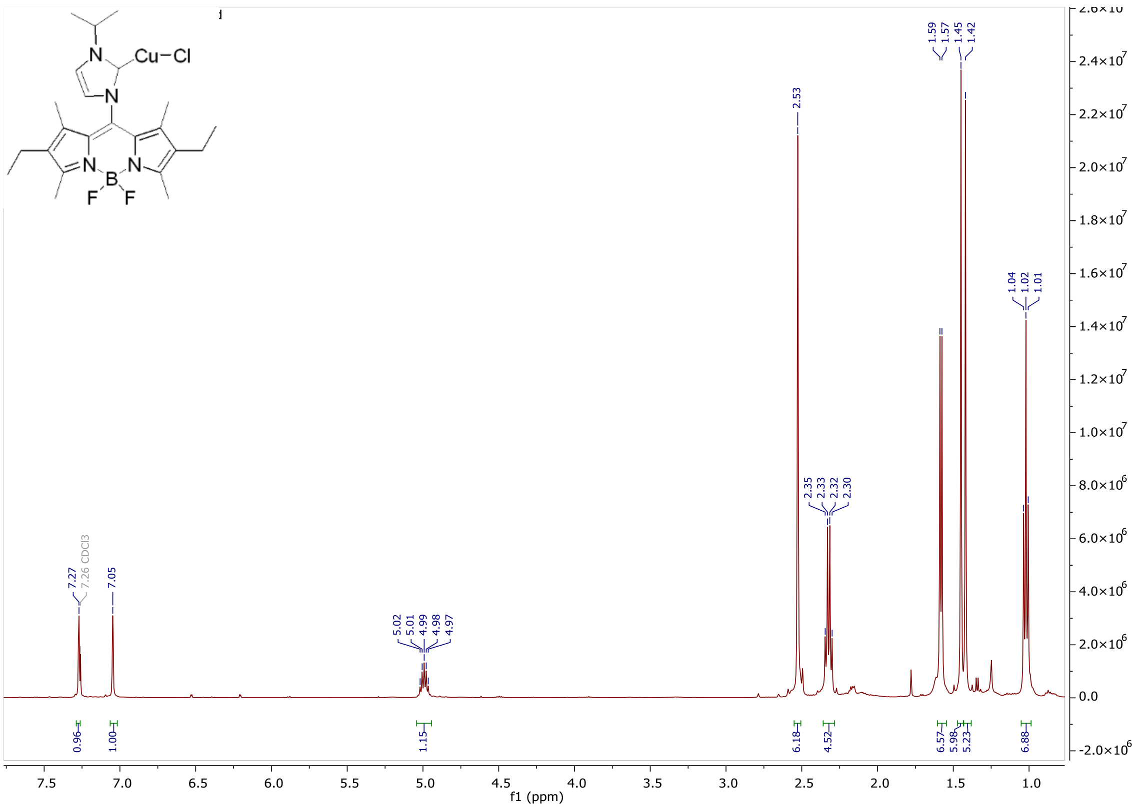

Figure S48. ^{1}H-NMR (500 MHz) of [CuCl(**3**)] complex in $CDCl_3$.

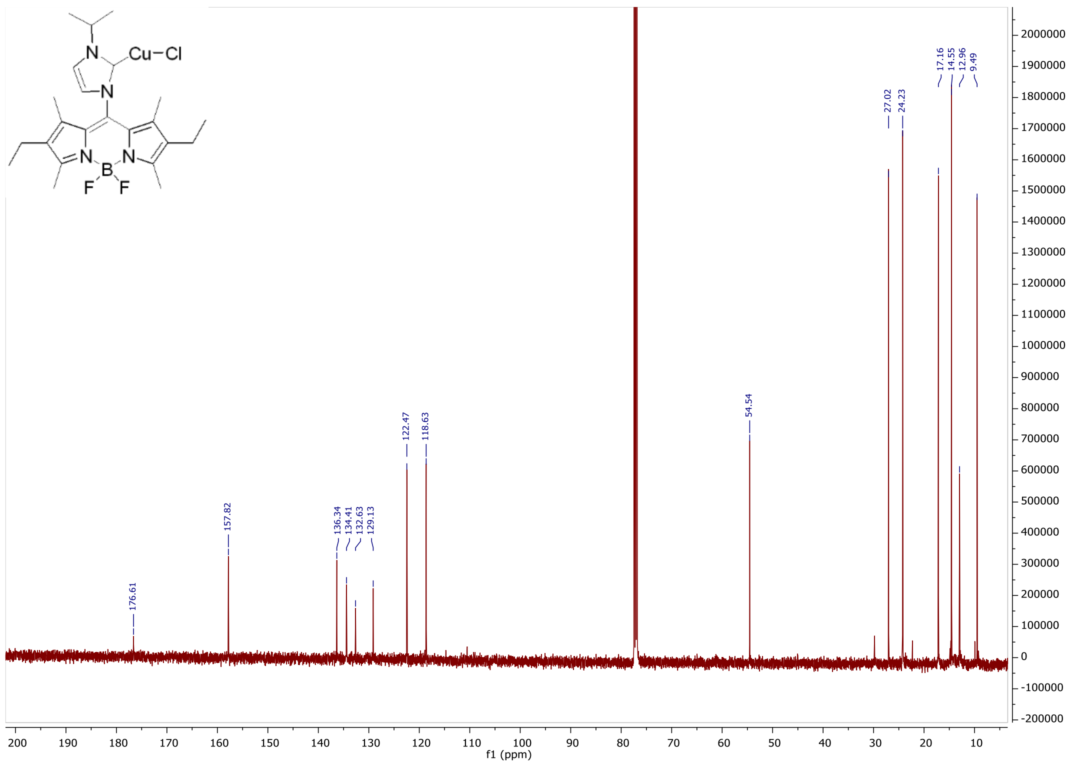

Figure S49. $^{13}C\{^1H\}$-NMR (126 MHz) of [CuCl(**3**)] complex in $CDCl_3$.

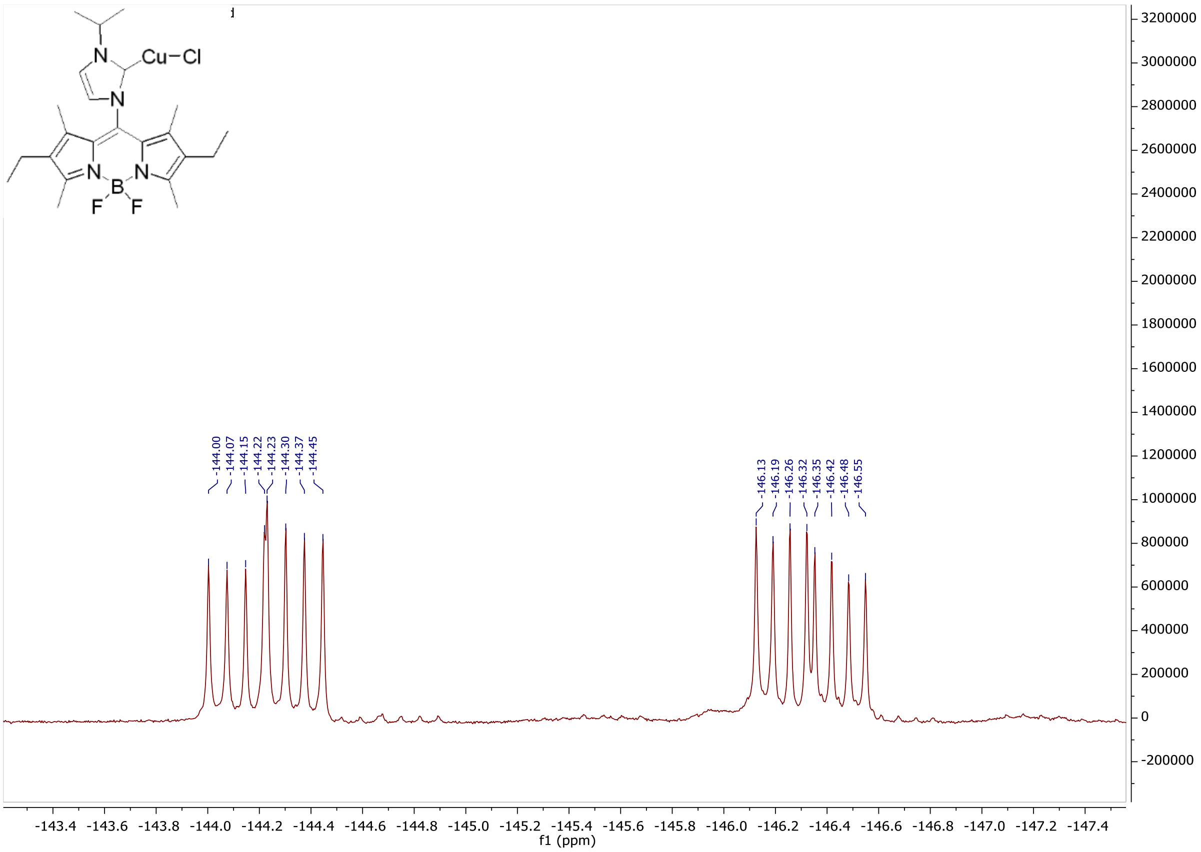

Figure S50. ^{19}F-NMR (471 MHz) of [CuCl(**3**)] complex in $CDCl_3$.

IR spectra

IR spectra of the metal carbonyls were recorded on a Fisher Scientific Nicolet 6700 FT-IR spectrometer in 1,2-dichloroethane solution using the ATR method with germanium prism in the corresponding accessory. (IC department)

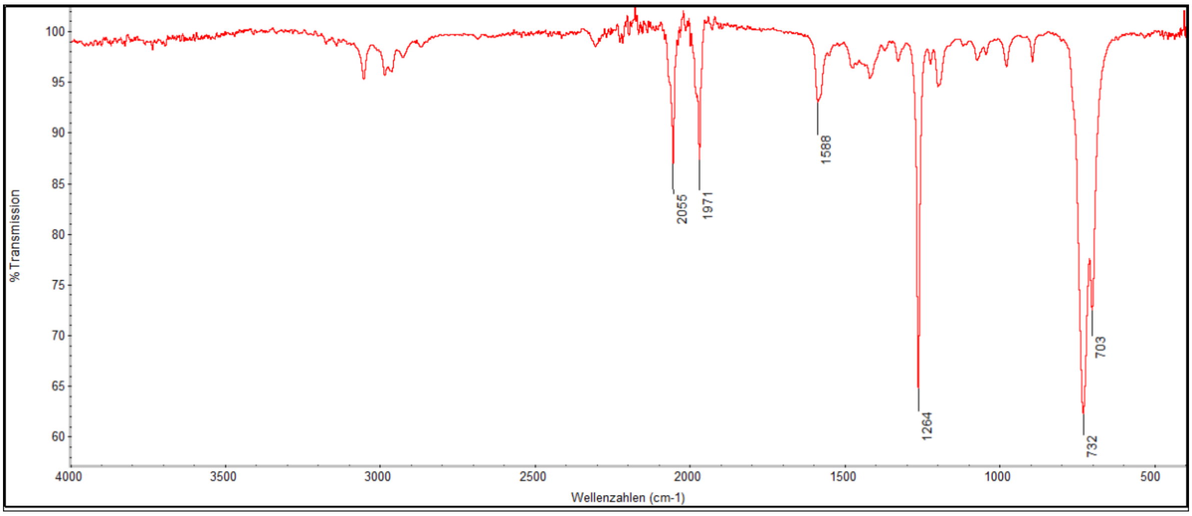

Figure S51. IR spectrum of [IrCl(CO)$_2$(**3**)] complex.

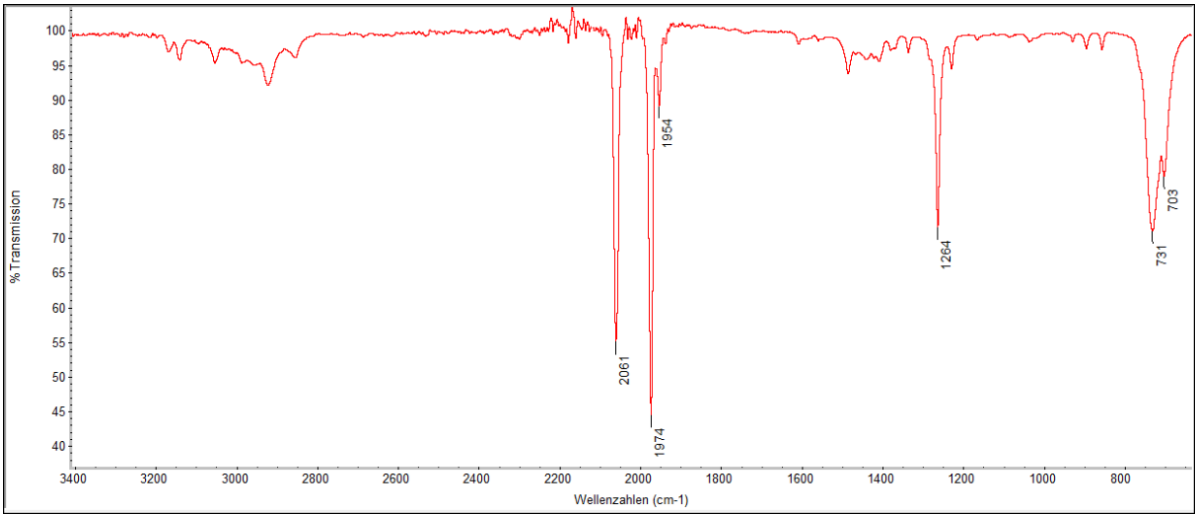

Figure S52. IR spectrum of [IrCl(CO)$_2$(**IMes**)] complex.

IR spectra of the metal carbonyls were recorded on an FT-IR Perkin-Elmer spectrometer in $CDCl_3$ solution using the ATR method with UATR Diamond/ZnSe ATR accessory. (OC department)

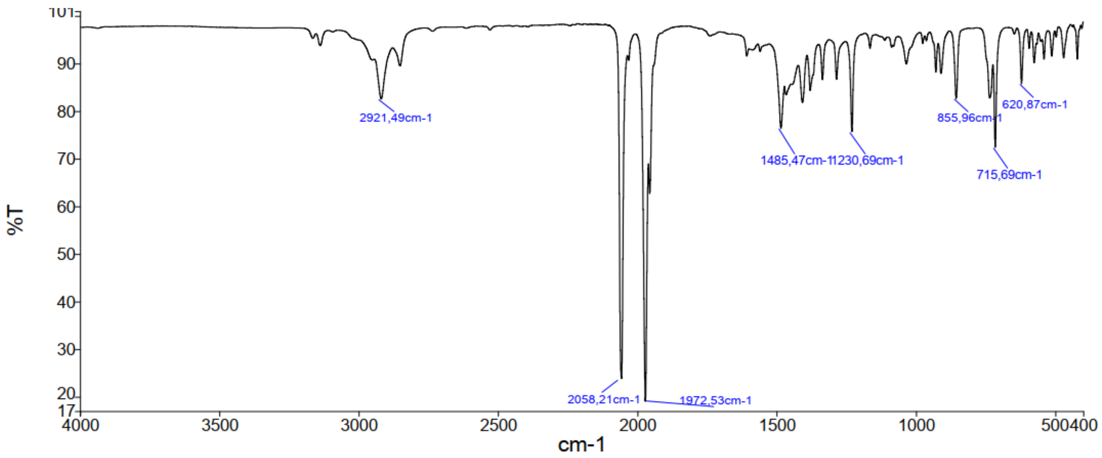

Figure S53. IR spectrum of [IrCl(CO)$_2$(**IMes**)] complex (data from this spectrometer not used in the discussion)

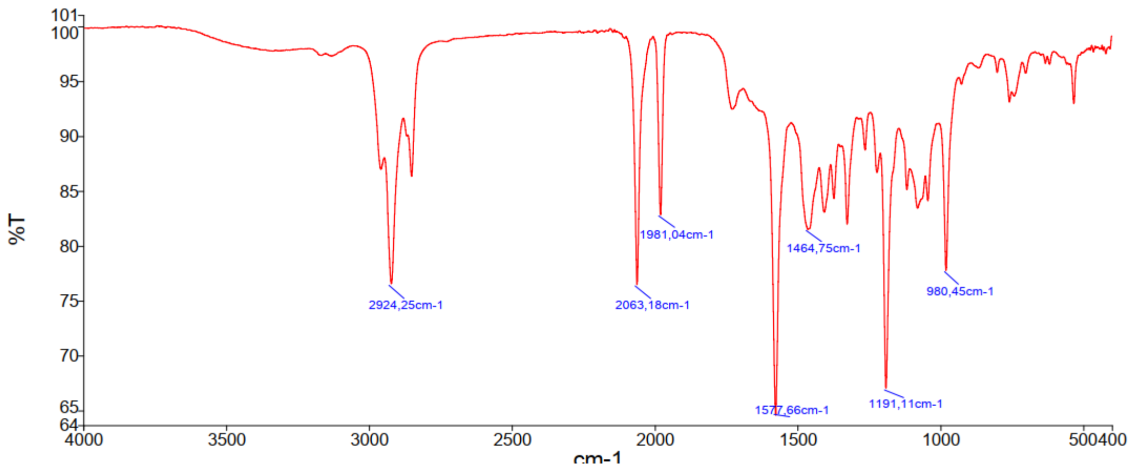

Figure S54. IR spectrum of [IrCl(CO)$_2$(**3**)] complex. (data from this spectrometer not used in the discussion)

Cyclic voltammetry

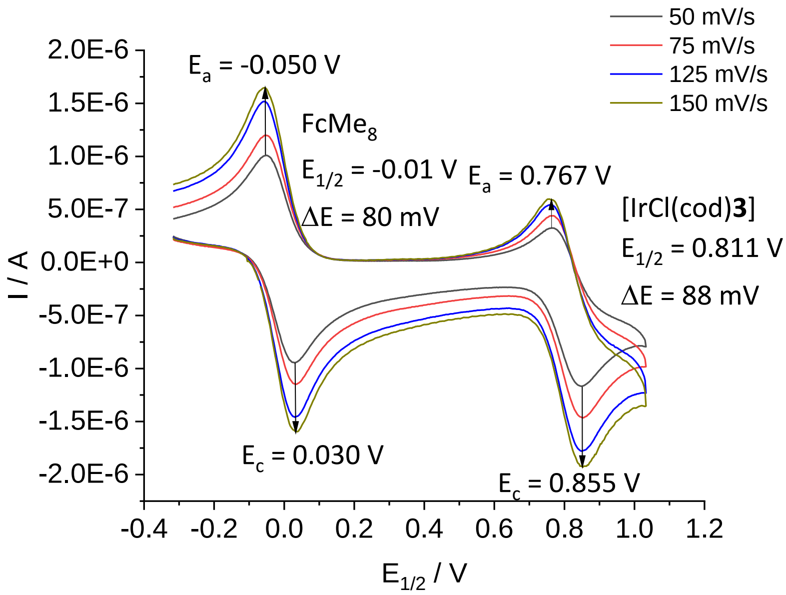

Figure S55a. Cyclic voltammogram of [IrCl(cod)(**3**)] was recorded in dry methylene chloride under an atmosphere of argon, supporting electrolyte N*n*Bu$_4$PF$_6$ (*c* = 0.1 mol/L) at variable scan rate referenced vs Fc/Fc$^+$.

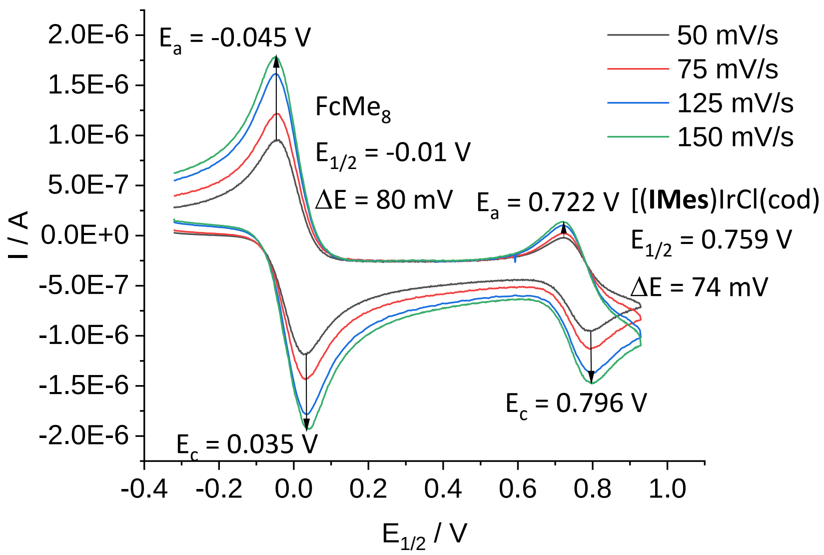

Figure S56b. Cyclic voltammogram of [IrCl(cod)(IMes)] was recorded in dry methylene chloride under an atmosphere of argon, vs. FcMe$_8$, supporting electrolyte N*n*Bu$_4$PF$_6$ (*c* = 0.1 mol/L) at variable scan rate.

Mass spectrometry data

Analysis	D:\Data\Plenio\87565_ESI_HR_P1-E-3_01_14215.d	Acquisition Date	15.12.2021 15:34:02
Sample Name	87565_ESI_HR	Ionisation	ESI Positive
Method	as 50-1600 1hz.m	Mass Range	50 m/z - 1600 m/z
Client	Popov BODIPY-imidazole SP	Operator	Rudolph

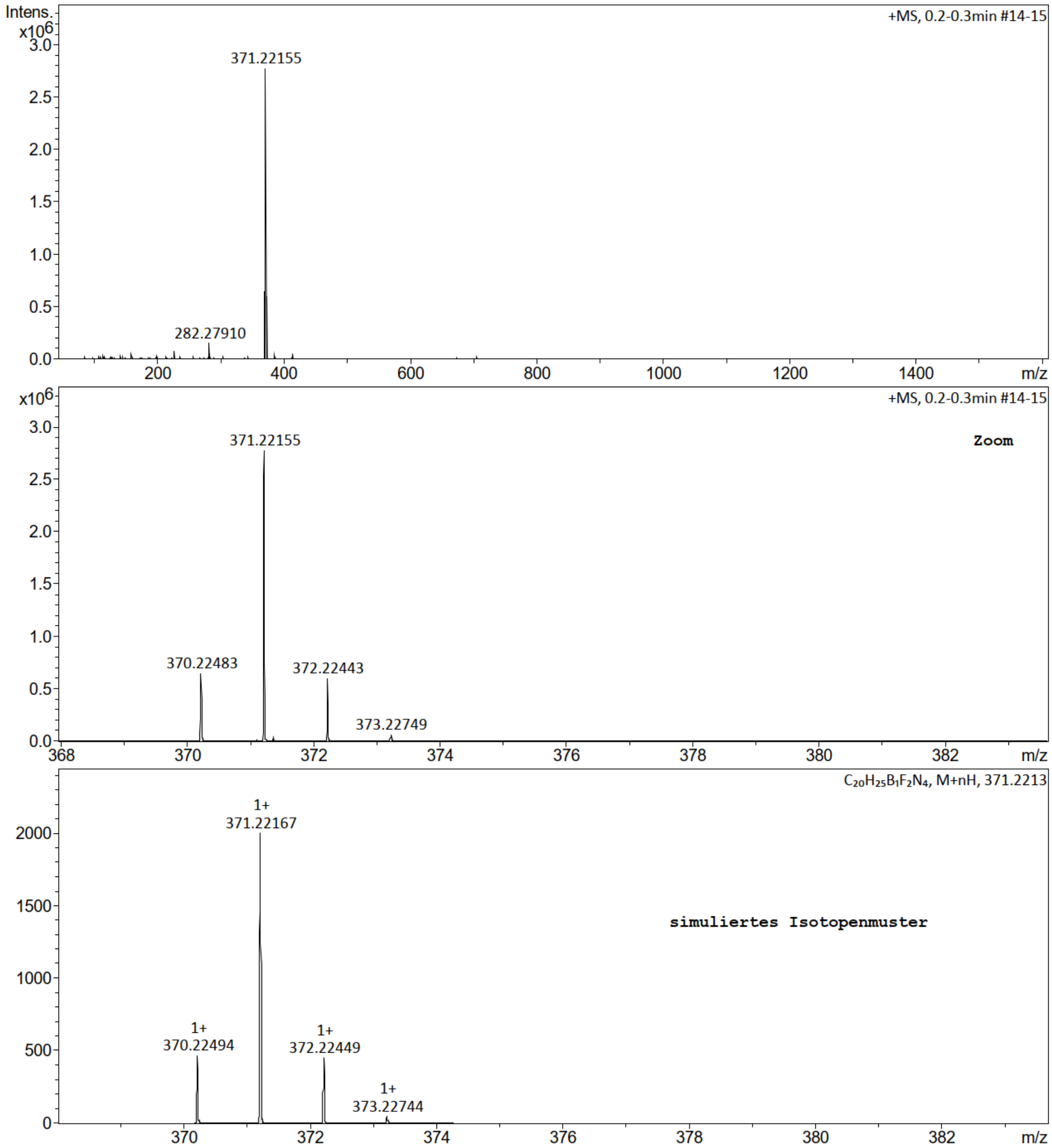

Mass Spectrometry Facility, Department of Chemistry, Technische Universität Darmstadt Instrument: Bruker Impact II

Page 1 of 2

#	Meas. m/z	m/z	Ion Formula	Adduct	Sum Formula	|err| [mDa]	|err| [ppm]	mSigma	e⁻ Conf	z
1	371.22155	371.22131	C20H26BF2N4	M+H	C20H25BF2N4	0.12	0.33	4.8	even	1+

Accurate Mass Measurement

Figure S57. Mass spectra of 8-imidazolo BODIPY (**2**).

Analysis	D:\Data\Plenio\87564_ESI_HR_P1-E-2_01_14214.d	Acquisition Date	15.12.2021 15:32:31
Sample Name	87564_ESI_HR	Ionisation	ESI Positive
Method	as 50-1600 1hz.m	Mass Range	50 m/z - 1600 m/z
Client	Popov BODIPY-imid.iodid SP	Operator	Rudolph

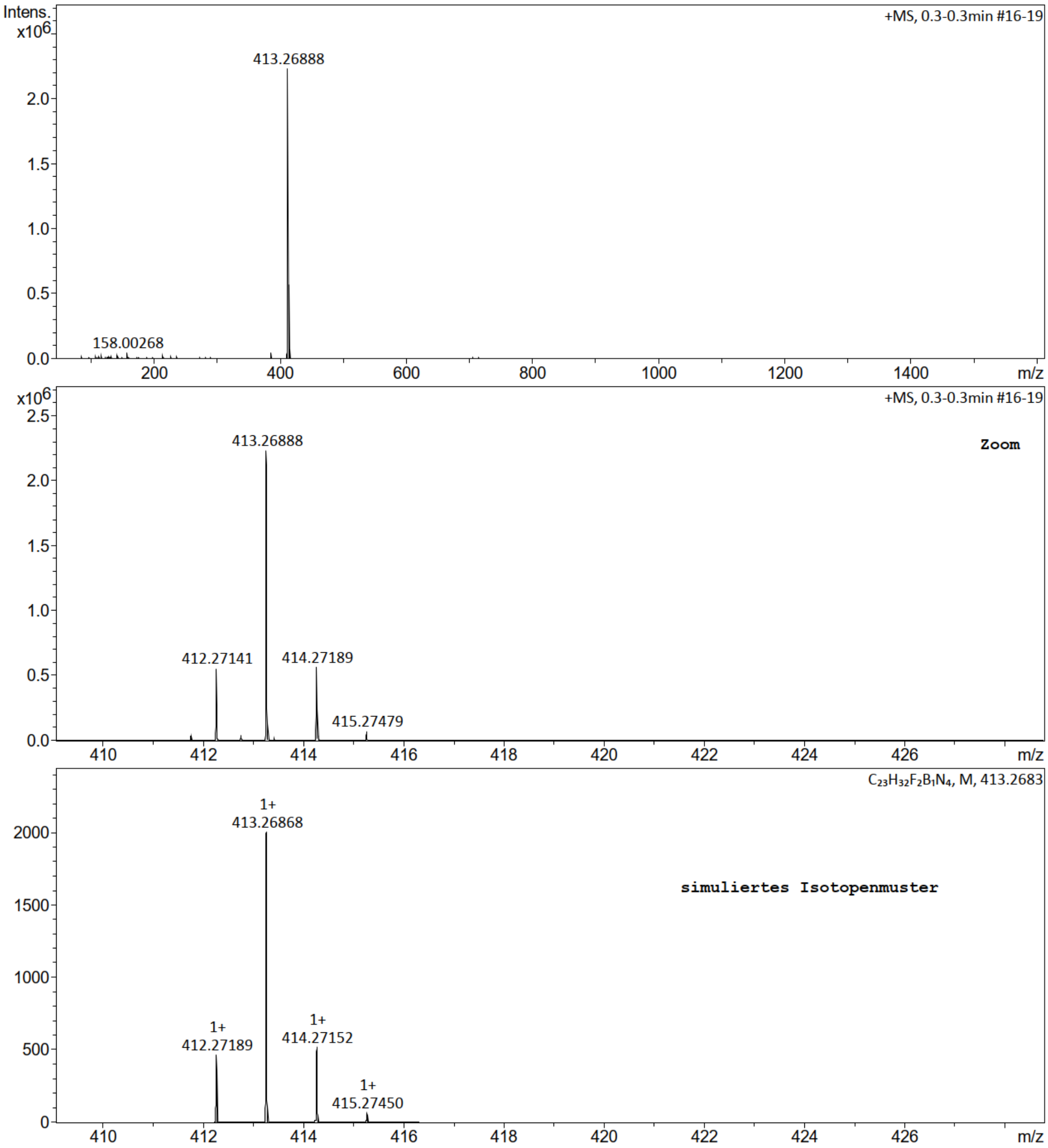

Mass Spectrometry Facility, Department of Chemistry, Technische Universität Darmstadt Instrument: Bruker Impact II

#	Meas. m/z	m/z	Ion Formula	Adduct	Sum Formula	|err| [mDa]	|err| [ppm]	mSigma	e⁻ Conf	z
1	413.26888	413.26826	C23H32BF2N4	M	C23H32BF2N4	0.20	0.49	8.3	even	1+

Accurate Mass Measurement

gef.: M-Jod

Figure S58. Mass spectra of BODIPY imidazolium salt (**3**)

Accurate Mass Measurement

Analysis	D:\Data\Plenio\86733_APCI_HR_P1-D-1_01_11212.d	Acquisition Date	28.07.2021 14:30:13
Sample Name	86733_APCI_HR	Ionisation	APCI Positive
Method	apci_pos_1600.m	Mass Range	50 m/z - 1600 m/z
Client	Popov SP-NHC (AuCl)	Operator	rudolph

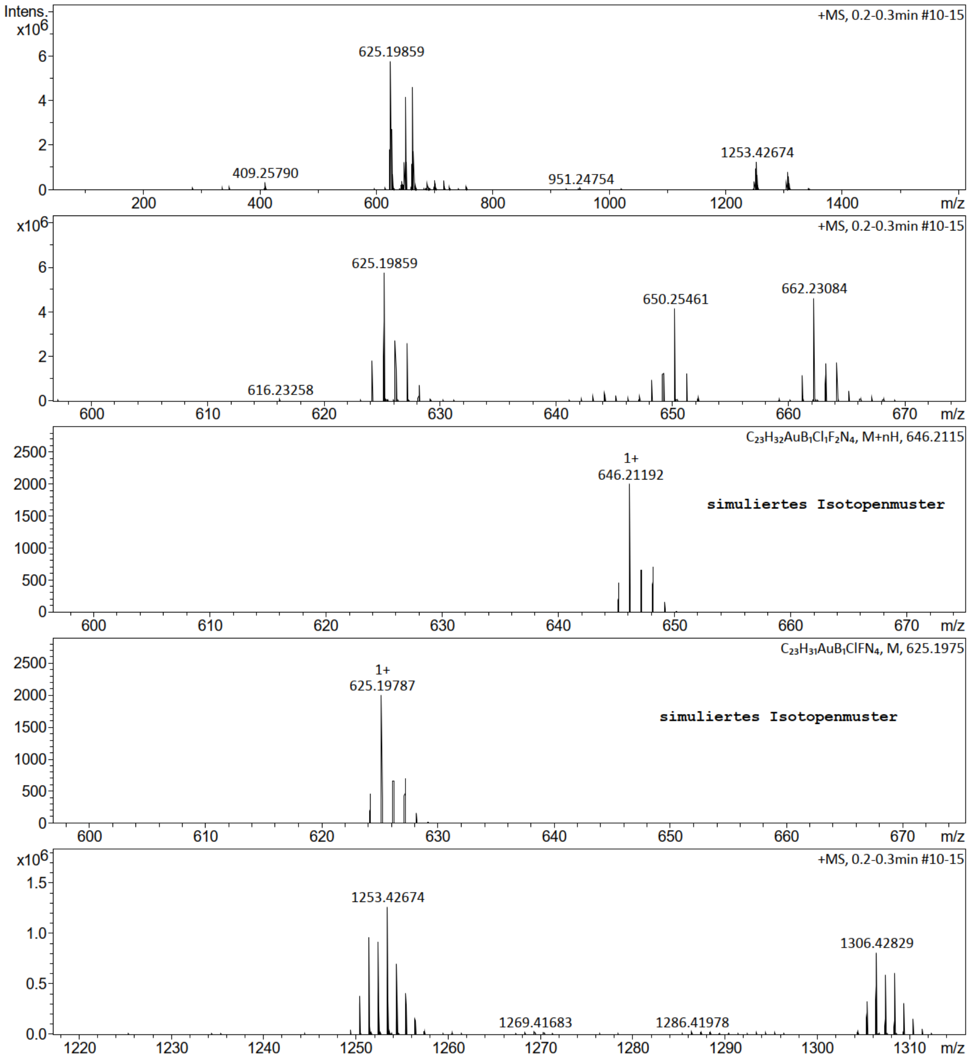

Mass Spectrometry Facility, Department of Chemistry, Technische Universität Darmstadt Instrument: Bruker Impact II

Page 1 of 2

Accurate Mass Measurement

#	Meas. m/z	Ion Formula	m/z	Sum Formula	|err| [mDa]	err [ppm]	e⁻ Conf	Adduct	z
1	625.19859	C28H32AuBClN	625.19765	C28H32AuBClN	0.44	-0.71	odd	M	1+
1	650.25461	C25H34AuBF2N5	650.25355	C25H34AuBF2N5	0.61	-0.94	even	M	1+
1	662.23084	C28H36AuBClFN2	662.23043	C28H36AuBClFN2	0.09	0.13	odd	M	1+
1	662.23084	C28H36AuBClFN2	662.23043	C28H32AuBClFN	0.09	0.13	odd	M+NH4	1+
2	625.19859	C23H31AuBClFN4	625.19745	C23H31AuBClFN4	0.72	-1.16	even	M	1+
2	650.25461	C30H35AuBFN2	650.25375	C30H35AuBFN2	0.33	-0.51	odd	M	1+
2	662.23084	C23H35AuBClF2N5	662.23023	C23H35AuBClF2N5	0.19	-0.29	even	M	1+
2	662.23084	C23H35AuBClF2N5	662.23023	C23H31AuBClF2N4	0.19	-0.29	even	M+NH4	1+

Summenformel Auftragsformular C23H32AuBClF2N4 = 645g/mol

Figure S59. Mass spectra of [AuCl(**3**)].

Accurate Mass Measurement

Analysis	D:\Data\Plenio\86190_ESI_HR_P1-D-1_01_9541.d	Acquisition Date	13.04.2021 16:59:57
Sample Name	86190_ESI_HR	Ionisation	ESI Positive
Method	as 50-1500 1hz.m	Mass Range	50 m/z - 1600 m/z
Client	Popov bdp_NHC_Ir_cod_Cl	Operator	Rudolph

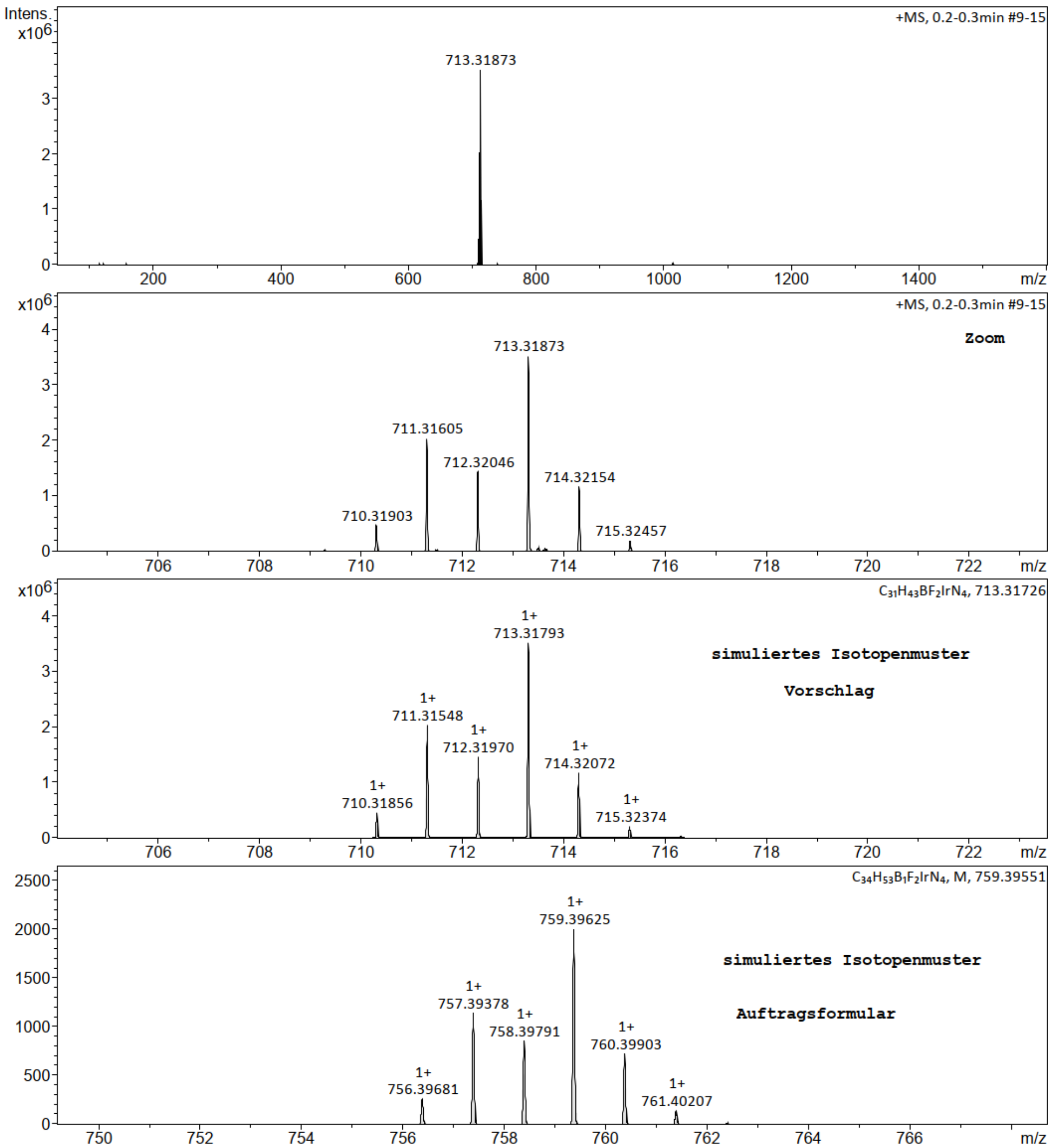

Mass Spectrometry Facility, Department of Chemistry, Technische Universität Darmstadt Instrument: Bruker Impact II

Accurate Mass Measurement

#	Meas. m/z	Ion Formula	m/z	Sum Formula	|err| [mDa]	err [ppm]	e⁻ Conf	Adduct	z
1	713.31873	C31H43BF2IrN4	713.31726	C31H43BF2IrN4	0.80	-1.12	even	M	1+
1	713.31873	C31H43BF2IrN4	713.31726	C31H42BF2IrN4	0.80	-1.12	even	M+H	1+

Figure S60. Mass spectra of [IrCl(cod)(**3**)].

Accurate Mass Measurement

Analysis	D:\Data\Plenio\86189_ESI_HR_P1-D-1_01_9540.d	Acquisition Date	13.04.2021 12:40:57
Sample Name	86189_ESI_HR	Ionisation	ESI Positive
Method	as 50-1500 1hz.m	Mass Range	50 m/z - 1600 m/z
Client	Popov bdp_NHC_Rh_cod_Cl	Operator	Rudolph

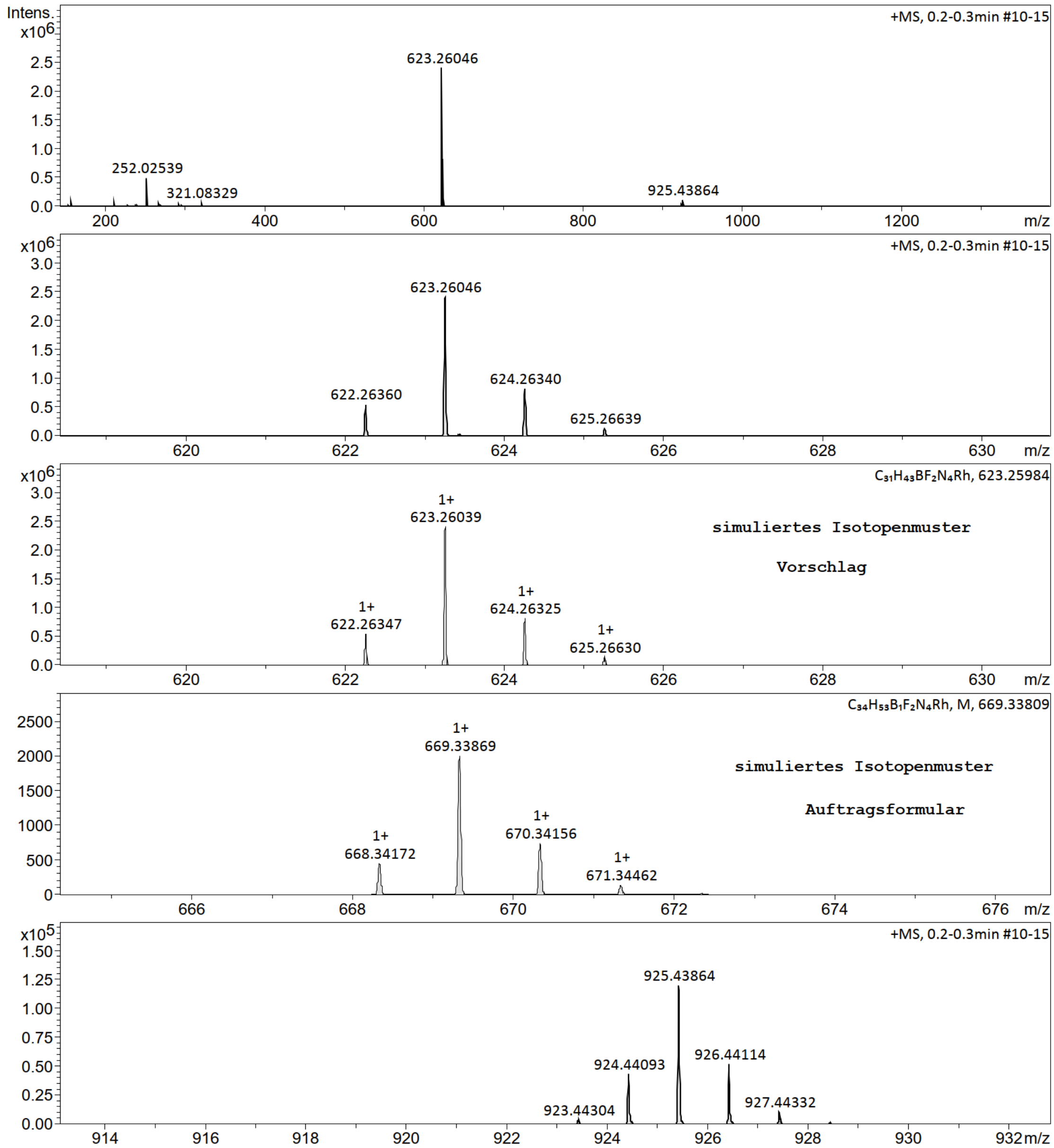

Mass Spectrometry Facility, Department of Chemistry, Technische Universität Darmstadt Instrument: Bruker Impact II

Page 1 of 2

Accurate Mass Measurement

#	Meas. m/z	Ion Formula	m/z	Sum Formula	|err| [mDa]	err [ppm]	e⁻ Conf	Adduct	z
1	623.26046	C31H43BF2N4Rh	623.25984	C31H43BF2N4Rh	0.07	-0.12	even	M	1+
1	623.26046	C31H43BF2N4Rh	623.25984	C31H42BF2N4Rh	0.07	-0.12	even	M+H	1+

Figure S61. Mass spectra of [RhCl(cod)(**3**)].

Accurate Mass Measurement

Analysis	D:\Data\Plenio\86734_ESI_HR_P1-D-2_01_11209.d	Acquisition Date	28.07.2021 13:34:49
Sample Name	86734_ESI_HR	Ionisation	ESI Positive
Method	as 50-1600 1hz.m	Mass Range	50 m/z - 1600 m/z
Client	Popov SP-NHC (Pd(allyl)Cl)	Operator	rudolph

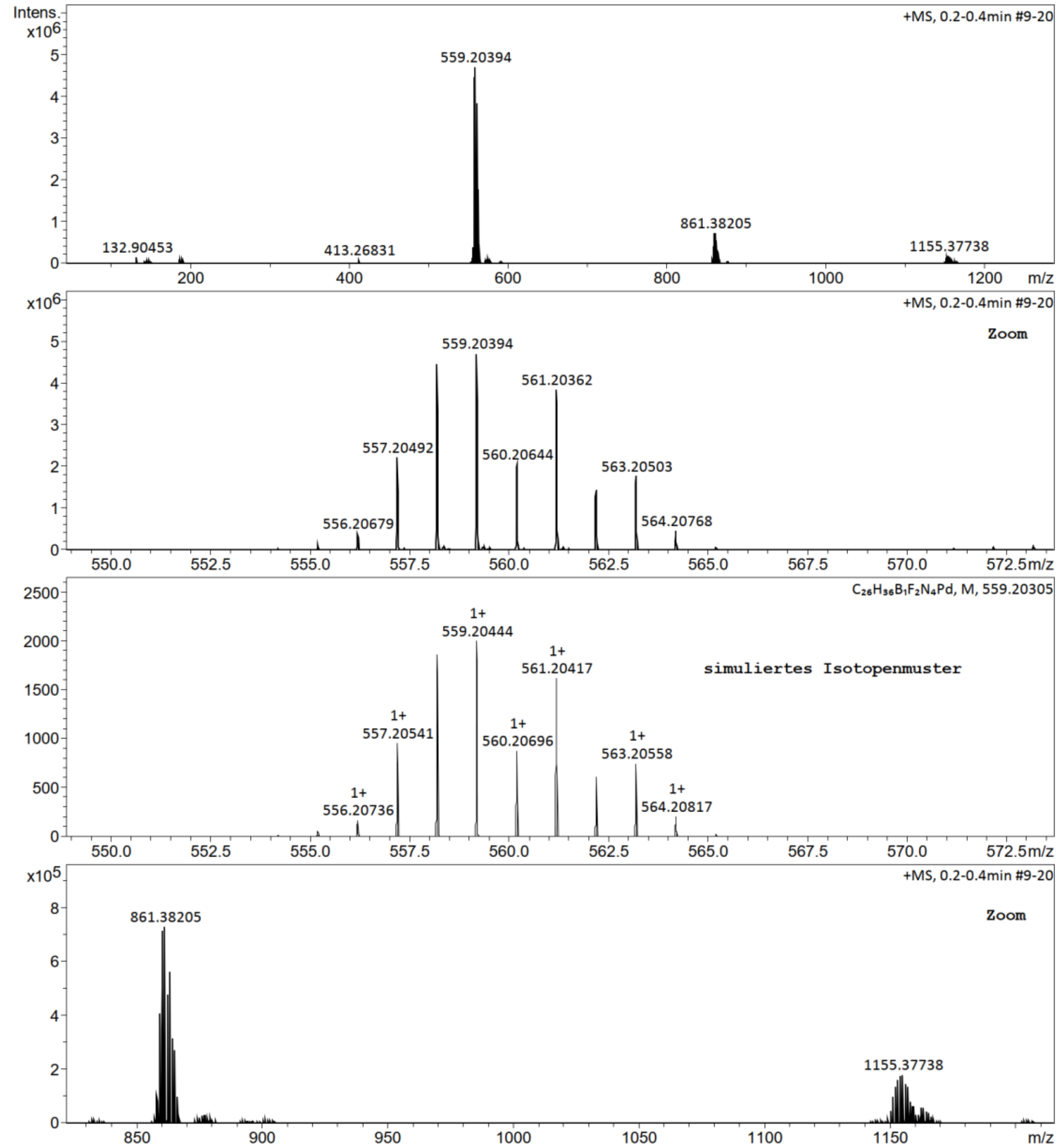

Mass Spectrometry Facility, Department of Chemistry, Technische Universität Darmstadt   Instrument: Bruker Impact II

Page 1 of 2

Accurate Mass Measurement

#	Meas. m/z	Ion Formula	m/z	Sum Formula	|err| [mDa]	err [ppm]	e⁻ Conf	Adduct	z
1	559.20394	C26H36BF2N4Pd	559.20305	C26H36BF2N4Pd	0.49	0.88	even	M	1+

Figure S62. Mass spectra of [PdCl(allyl)(**3**)].

Accurate Mass Measurement

Analysis	D:\Data\Plenio\88021_ESI_HR_P1-C-3_01_15657.d	Acquisition Date	16.02.2022 14:50:09
Sample Name	88021_ESI_HR	Ionisation	ESI Positive
Method	as 50-1600 1hz.m	Mass Range	50 m/z - 1600 m/z
Client	Popov IrClCO2-NHC-Bodipy-SP	Operator	Rudolph

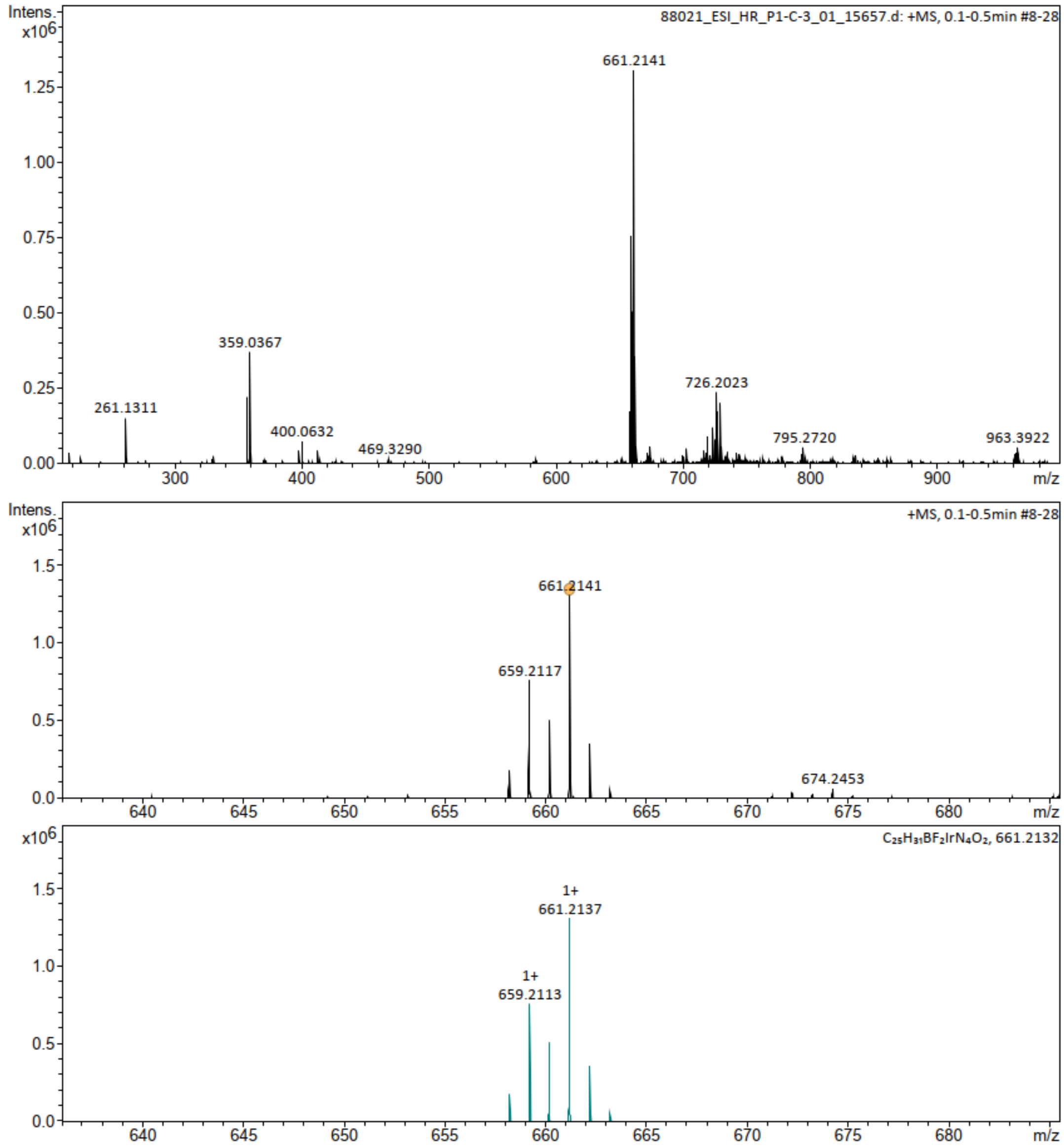

Mass Spectrometry Facility, Department of Chemistry, Technische Universität Darmstadt Instrument: Bruker Impact II

Page 1 of 2

Accurate Mass Measurement

Meas. m/z	#	Ion Formula	m/z	err [ppm]	mSigma	# mSigma	Score	rdb	e⁻ Conf	N-Rule
661.2141	1	C25H31BF2IrN4O2	661.2132	-0.6	2.5	1	100.00	12.5	even	ok
	2	C29H32IrN4O2	661.2149	1.4	90.6	2	4.76	16.5	even	ok
	3	C46H28BF2O2	661.2145	1.7	122.2	3	0.86	32.5	even	ok
	4	C49H27BFO	661.2134	0.1	133.8	4	0.76	36.5	even	ok

Figure S63. Mass spectra of [IrCl(CO)$_2$(**3**)].

Accurate Mass Measurement

Analysis	D:\Data\Plenio\88020_ESI_HR_P1-C-2_01_15656.d	Acquisition Date	16.02.2022 14:45:11
Sample Name	88020_ESI_HR	Ionisation	ESI Positive
Method	as 50-1600 1hz.m	Mass Range	50 m/z - 1600 m/z
Client	Popov RhClCO2-NHC-Bodipy-SP	Operator	Rudolph

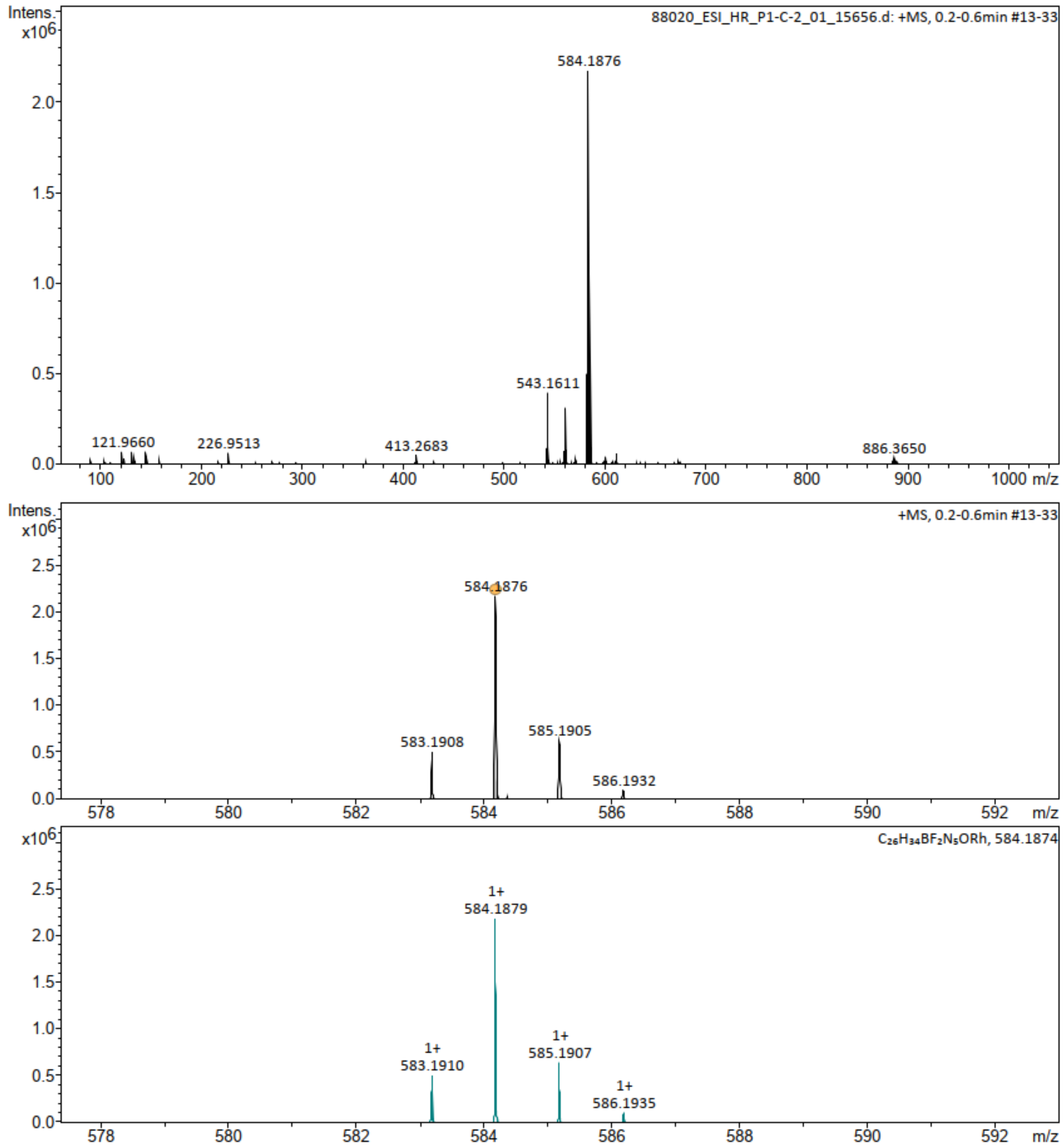

Mass Spectrometry Facility, Department of Chemistry, Technische Universität Darmstadt Instrument: Bruker Impact II

Page 1 of 2

Accurate Mass Measurement

Meas. m/z	#	Ion Formula	m/z	err [ppm]	mSigma	# mSigma	Score	rdb	e⁻ Conf	N-Rule
584.1876	1	C26H34BF2N5ORh	584.1874	0.5	2.1	1	100.00	12.5	even	ok
	2	C38H23FN5O	584.1881	0.9	75.8	2	11.94	29.5	even	ok
	3	C41H22N5	584.1870	-1.1	93.0	3	5.51	33.5	even	ok

Figure S64. Mass spectra of [RhCl(CO)$_2$(**3**)].

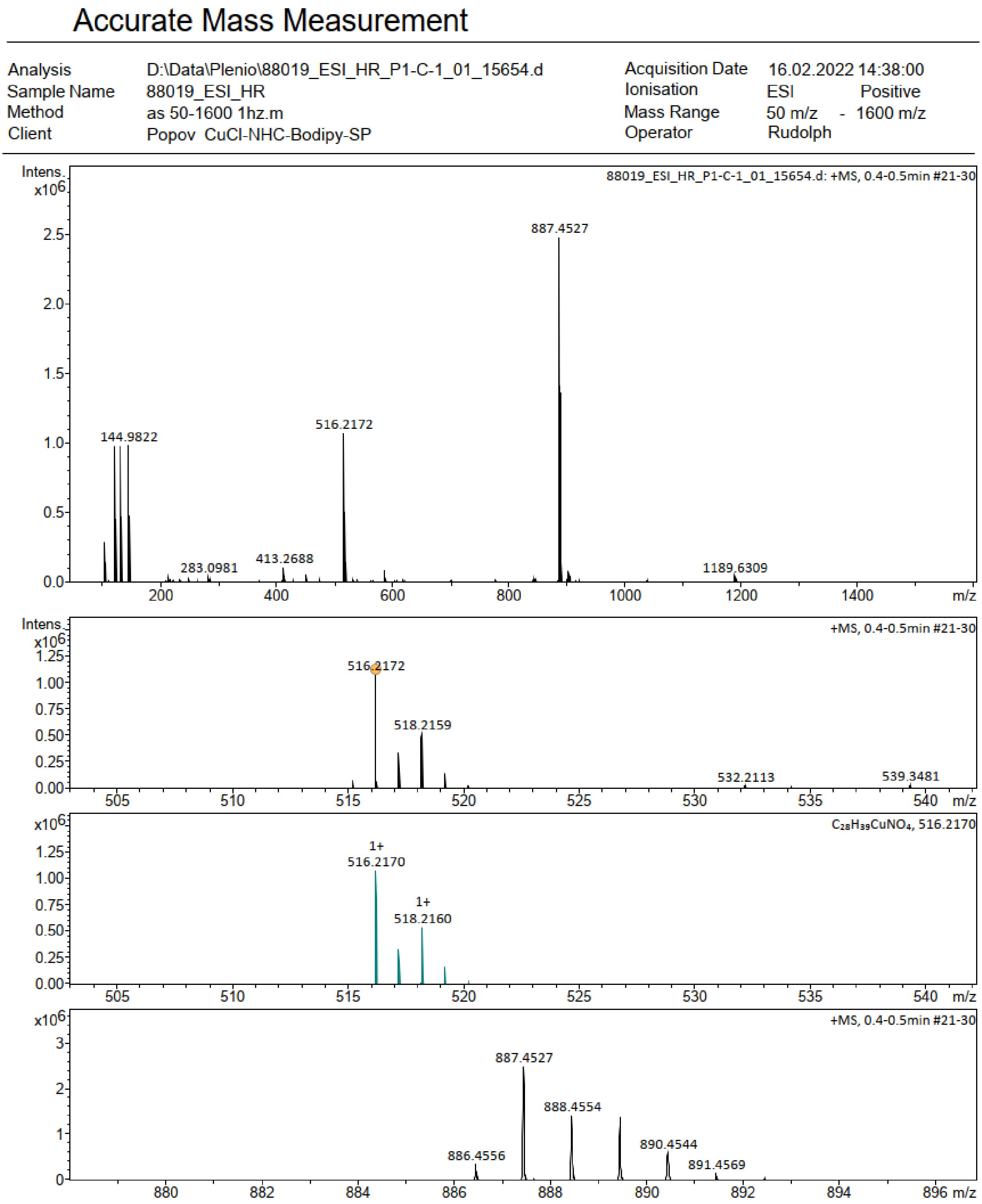

Figure S65. Mass spectra of [CuCl(**3**)].

Crystal structure data

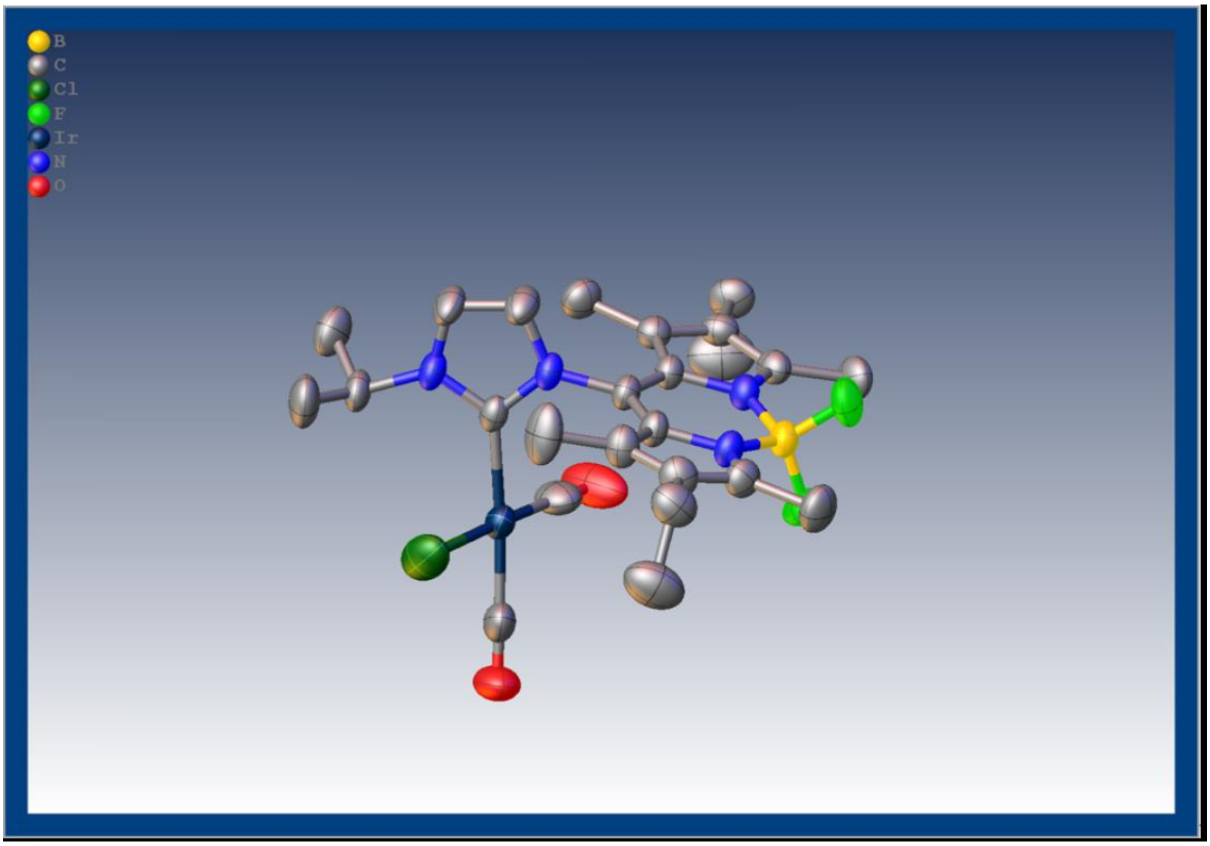

Table S1. Crystal data and structure refinement for [IrCl(CO)$_2$(**3**)].

Identification code	[IrCl(CO)$_2$(**3**)]
Empirical formula	$C_{25}H_{32}BClF_2IrN_4O_2$
Formula weight	697.00
Temperature/K	293(2)
Crystal system	triclinic
Space group	P-1
a/Å	8.9881(4)
b/Å	10.8888(5)
c/Å	14.4922(7)
α/°	87.662(4)
β/°	81.638(4)

γ/°	76.400(4)
Volume/Å^3	1363.89(11)
Z	1
ρ_{calc}g/cm^3	0.849
μ/mm^{-1}	2.518
F(000)	343.0
Crystal size/mm^3	0.4 × 0.16 × 0.16
Radiation	MoKα (λ = 0.71073)
2Θ range for data collection/°	5.148 to 56.16
Index ranges	-9 ≤ h ≤ 11, -9 ≤ k ≤ 13, -18 ≤ l ≤ 18
Reflections collected	10240
Independent reflections	5970 [R_{int} = 0.0203, R_{sigma} = 0.0415]
Data/restraints/parameters	5970/0/333
Goodness-of-fit on F^2	1.048
Final R indexes [I>=2σ (I)]	R_1 = 0.0319, wR_2 = 0.0571
Final R indexes [all data]	R_1 = 0.0474, wR_2 = 0.0627
Largest diff. peak/hole / e Å^{-3}	0.72/-0.74

Experimental Single crystals of $C_{25}H_{32}BClF_2IrN_4O_2$ [IrCl(CO)$_2$(**3**)] were grown by cooling a pentane/CH_2Cl_2 solution of the complex. A suitable crystal was selected and kept at 293(2) K during data collection.

References

[1] P. Irmler, F. Gogesch, A. Mang, M. Bodensteiner, C. Larsen, O. Wenger and R. Winter, *Dalton Trans.*, **2019**, *48*, 11690-11705;